Supplemental Figure Legends

Supplemental Figure 1

(A) Changes in molecules involved in cAMP signaling. β_1-Adrenergic receptor (AR), β_2-AR, β-adrenergic receptor kinase (βARK), Gsα, Giα, Gβ, Gq, PKA subunits (catalytic (cat), regulatory IIα subunit (RIIα) and regulatory Iα subunits (RIα)) in addition to type 5/6 adenylyl cyclase, Epac2 in WT (wild-type control) and Epac1KO (Epac1 null mice).

(B) Northern blotting of Epac1, Epac2 and GAPDH in heart of WT and Epac1KO.

Supplemental Figure 2

Response of left ventricular ejection fraction (LVEF) and left ventricular end-diastolic diameter (LVESD) to ISO in vivo.

(A) LVEF was significantly decreased in Epac1KO versus WT, but the increase of LVEF in response to β-AR stimulation with intravenous ISO infusion (0, 0.13, 0.27, 0.40 μg/kg/min for 5 minutes) was not altered in Epac1KO (n = 4-7, *P < 0.01).

(B) LVESD was significantly increased in Epac1KO versus WT, but the decrease of LVESD in response to β-AR stimulation with intravenous ISO infusion (0, 0.13, 0.27, 0.40 μg/kg/min for 5 minutes) was not altered in Epac1KO (n = 4-7, *P < 0.01).

Supplemental Figure 3

Contractility of isolated myocardium in Epac1KO

(A) The contractility of isolated myocardium of Epac1KO was compared with that of

WT. The basal contractile force was significantly smaller in Epac1KO mice than that in WT controls (WT versus Epac1KO: 112 $\pm$ 14.7 versus 73 $\pm$ 7.1 mg/mm^2, n = 6-7, *P < 0.05). ISO enhanced the contractile force dose-dependently in both WT and Epac1KO.

(B) The magnitude of the increase in response to ISO, as evaluated by change in contractile force, was similar in WT and Epac1KO. The sensitivity to β-adrenergic stimulation with ISO was almost the same in Epac1KO and WT; the –log EC_{50} value for the enhancement of contractile force with ISO was 7.04 $\pm$ 0.07 in WT and 7.06 $\pm$ 0.11 in Epac1KO, P = NS, *not significant*, n = 6-7).

(C) The time required to reach peak tension was similar in Epac1KO and WT at baseline (WT versus Epac1KO ; 50 $\pm$ 1.1 versus 52 $\pm$ 1.5 msec, n = 6-7, P = NS, *not significant*) and the tension subsequently decreased similarly in WT and Epac1KO.

(D) The time required for 90% relaxation was significantly longer in Epac1KO at baseline (WT versus Epac1KO: 54 $\pm$ 1.5 versus 61 $\pm$ 2.0 msec, n = 6-7, *P < 0.05), but it became similar in Epac1KO and WT in response to ISO.

Supplemental Figure 4

Immunoblotting to show phosphorylation on threonine-286 of CaMKII in the heart of WT and Epac1KO at baseline.

Phosphorylation on threonine-286 (Thr 286) of CaMKII showed no difference between Epac1KO and WT at baseline (WT versus Epac1KO: 100 $\pm$ 9.8 versus 103 $\pm$ 17%, n = 6, P = NS, *not significant*). The ratio of phosphorylated/total protein expression on Thr-286 of CaMKII in WT heart at baseline was taken as 100% in each determination. *Inserts*; representative immunoblotting results are shown.

Supplemental Figure 5

Efffects of Epac activation on phospholamban (PLN) phosphorylation at serine 16 (Ser16) in neonatal mouse cardiac myocytes prepared from WT and Epac1KO. Epac activation with 8-CPT-AM (1 μM for 15 min) significantly increased PLN phosphorylation at serine-16 from baseline in WT, and the level was also significantly greater than that of Epac1KO (*P < 0.05). In contrast to WT, it only tended to increase the phosphorylation in Epac1KO but not significant (WT: from 100 $\pm$ 11 to 1534 $\pm$ 528%, **P < 0.01, n = 4-6; Epac1KO: from 61 $\pm$ 22 to 476 $\pm$ 141%, n = 4-6, P = NS, *not significant*). The ratio of serine-16 phosphorylated/total protein expression of phospholamban at baseline was taken as 100% in each determination. T-PLN, total phospholamban; p-PLN, phosphorylated PLN. *Inserts*; representative immunoblotting results are shown.

Supplemental Figure 6

Effects of PLC and PKC on Epac-mediated phosphorylation on serine-16 in neonatal

cardiac myocytes.

Epac-mediated phosphorylation of PLN on serine-16 with 8-CPT-AM (10 μM) for 2 hours (332 ± 47%) was significantly attenuated by the addition of PLC inhibitor (U73122 0.5 μM) (103 ± 11%) or PKC inhibitor (Ro-31-7549 1 μM) (105 ± 15%) (n = 4-11, *P < 0.01). The ratio of serine-16 phosphorylated/total protein expression of phospholamban at baseline was taken as 100% in each determination. T-PLN, total phospholamban; p-PLN, phosphorylated PLN. *Inserts*; representative immunoblotting results are shown.

Supplemental Figure 7

(A) Suppression of each subtype of PKC (α, β, δ, γ, ε) in cultured cardiomyocytes. Neonatal cardiomyocytes were transfected with 20 nM siRNAs to the selected region of each subtype as well as negative siRNA (si Control). At 24 hours after transfection, the level of mRNA of each subtype was quantified by real-time PCR (* P < 0.01 versus si Control, n = 4).

(B) Expression of each subtype of PKC (α, β, δ, γ, ε) was quantified by real-time PCR in cultured neonatal cardiac myocytes transfected with PKCε siRNA as well as negative siRNA (si Control) (* P < 0.01 versus si Control, n = 5-6).

Supplemental Figure 8

Epac-mediated PLN phosphorylation on serine-16 was examined in neonatal rat cardiac myocytes transfected with PKCα siRNA **(A)**, PKCβ siRNA **(B)**, PKCδ siRNA **(C)** PKCγ siRNA **(D)** or si Control for 24 hours. At 24 hours after transfection, cardiomyocytes were washed with serum-free medium, incubated for a further 24 hours, and treated with 8-CPT-AM (10 μM) for 2 hours. Then, PLN phosphorylation on serine-16 was examined by western blotting. PLN phosphorylation was significantly increased in cells transfected with both negative siRNA and siRNA of PKC subtype (α, β, δ, γ), but the magnitudes of the increase were similar in all cases (n = 4-8, P = NS, *not significant*). The ratio of phosphorylated/total protein expression of phospholamban in cells transfected with negative si RNA at baseline was taken as 100% in each determination. T-PLN, total PLN; p-PLN, phosphorylated PLN.

Supplemental Figure 9

Suppression of each subtype of Epac1 in cultured cardiomyocytes **(A)** and cardiofibroblasts **(B)**. Neonatal rat cardiomyocytes or cardiofibroblasts were transfected with 20 nM siRNAs to the selected region of Epac1 (si Epac1) as well as negative siRNA (si Control). At 24 hours after transfection, the level of Epac1 protein was quantified by immunoblotting (** $P < 0.01$ versus si Control, n = 4-5). *Inserts*; representative immunoblotting results are shown **(A)**.

Supplemental Figure 10

Effects of Ad-PKI-GFP infection on PLN phosphorylation on serine-16 and threonine-17 in neonatal cardiac myocytes transfected with negative or Epac1 siRNA.

(B) Neonatal rat cardiomyocytes were infected with Ad-GFP (Control) or Ad-PKI-GFP at MOI 100. More than 98% of cells appeared green and GFP fluorescence was evenly distributed in the cytoplasma.

(C) PLN phosphorylation on serine-16 was significantly increased in cells transfected with Ad-GFP or Ad-PKI-GFP in addition to control siRNA after ISO treatment (10 μM) for 10 min, but the magnitude of the increase was significantly smaller in cells transfected with Ad-PKI-GFP (Ad-GFP (lane 2) vs. Ad-Epac1-GFP (lane 4): 60 $\pm$ 2.6 vs. 45 $\pm$ 3.1-fold, $*P < 0.05$, $n = 4$). Also, transfection of Epac1 siRNA significantly decreased the ISO-promoted PLN phosphorylation on serine-16 in cells transfected with Ad-PKI-GFP (lane 5: 22 $\pm$ 0.6, $**P < 0.01$, $n = 4$), but KN-93 pretreatment (10 μM) for 30 min did not decrease ISO-promoted PLN phosphorylation on serine-16 in cells transfected with control siRNA (lane 6: 37 $\pm$ 3.1, P = NS, *not significant*, $n = 8$). The ratio of phosphorylated/total protein expression of PLN in cells transfected with Ad-GFP in addition to negative siRNA at baseline was taken as 1-fold in each determination. T-PLN, total phospholamban; p-PLN, phosphorylated phospholamban.

(D) PLN phosphorylation on threonine-17 was significantly increased in cells transfected with Ad-GFP or Ad-PKI-GFP in addition to control siRNA after ISO treatment (10 μM) for 10 min, but the magnitude of the increase was similar in both cases (Ad-GFP (lane 2) vs. Ad-Epac1-GFP (lane 4): 59 $\pm$ 0.04 vs. 56 $\pm$ 0.05-fold, P =

NS, *not significant*, $n = 8$). Transfection of Epac1 siRNA significantly decreased the ISO-promoted PLN phosphorylation on serine-16 in cells transfected with Ad-PKI-GFP (lane 5: 41 $\pm$ 0.04, $^{*}P < 0.05$, $n = 8$), but KN-93 pretreatment (10 μM) for 30 min abrogated the ISO-promoted PLN phosphorylation on serine-17 in cells transfected with control siRNA (lane 6: 1.4 $\pm$ 0.003, $^{**}P < 0.01$, $n = 8$).

The ratio of phosphorylated/total protein expression of PLN in cells transfected with Ad-GFP in addition to negative siRNA at baseline was taken as 1 in each determination. T-PLN, total PLN; p-PLN, phosphorylated PLN.

Inserts; representative immunoblotting results are shown **(A)**.

Supplemental Figure 11

Effects of Epac1 silencing on RyR2 phosphorylation on serine-2808 and serine-2814 in neonatal rat cardiac myocytes.

Epac-mediated RyR2 phosphorylation on serine-2808 was examined in neonatal rat cardiac myocytes transfected with Epac1 siRNA or negative siRNA control for 24 hours, then washed with serum-free medium and incubated for a further 24 hours. After the incubation, cells were treated with ISO (10 μM) for 3 min and RyR2 phosphorylation on serine-2808 **(B)** and serine 2814 **(C)** was evaluated by western blotting.

(B) RyR2 phosphorylation on serine-2808 was significantly increased in cells transfected with control or Epac1 siRNA from baseline (Control siRNA versus Epac1

siRNA 252 ± 8 versus 186 ± 12%, $^{**}P < 0.01$, $n = 6$), but the magnitudes of the increase were significantly smaller in cells transfected with Epac1 siRNA ($^{\#\#}P < 0.01$).

(C) RyR2 phosphorylations on serine-2814 was significantly increased in cells transfected with control siRNA (226 ± 13%, $^{**}P < 0.01$, $n = 6$), but it only tended to be increased (not significant) in cells transfected with Epac1 siRNA (170 ± 2%, P = NS, *not significant*, $n = 6$). Also, the magnitudes of the increase tended to be smaller in cells transfected with Epac1 siRNA (P = NS, *not significant*).

The ratio of phosphorylated/total protein expression of RyR2 in cells transfected with negative siRNA at baseline was taken as 100% in each determination. T-RyR2, total RyR2; p-RyR2, phosphorylated RyR2. *Inserts*; representative immunoblotting results are shown **(A)**.

Supplemental Figure 12

The L-type Ca^{2+} channel current (I_{CaL}) recorded from adult mouse ventricular myocytes.

(A) The current traces of I_{CaL} recorded in ventricular myocytes isolated from Epac1KO. The pulse protocol is shown at the top of the left panel.

(B) The current-voltage relationships recorded under control condition and in the presence of ISO at 10^{-7} M are summarized. The left and right panels show the results for WT ($n = 6$) and Epac1KO ($n = 6$), respectively.

Supplemental Figure 13

Na^+-Ca^{2+} exchanger current (I_{NCX}) was recorded in adult mouse ventricular myocytes.

(A) The current-voltage relationships of I_{NCX} measured in WT (n = 5) or Epac1KO (n = 4) were averaged and superimposed.

(B) Current densities of I_{NCX} shown in A were extracted at every 20 mV and plotted against voltages.

(C) Current densities of I_{NCX} measured at -100 mV and 50 mV were summarized as a bar graph (P = NS, *not significant*, n = 4-5).

Supplemental Figure 14

Changes in LV function after banding in WT and Epac1KO. Hemodynamic measurements of LV function were performed at 3 weeks after TAC and in sham-operated controls (Sham) in WT and Epac1KO.

(A to C) Max dP/dt was significantly decreased **(A)** and Min dP/dt LVEF was significantly increased **(B)** in WT, but not in Epac1KO at 3 weeks after TAC (n = 13-18, $^{**}P < 0.01$, P = NS, *not significant*). End-diastolic pressure (EDP) was significantly increased in both WT and Epac1KO, but the magnitude of the increase was smaller in Epac1KO than that in WT **(C)** (n = 13-22, $^{*}P < 0.05$, $^{**}P < 0.01$).

(D to F) Changes of Max dP/dt **(D)**, Min dP/dT **(E)**, and EDP **(F)** from sham-operated controls at 3 weeks after banding were significantly greater in WT than in Epac1KO (*n* = 13-16, **P* < 0.05, ***P* < 0.01).

Supplemental Figure 15

Changes in cardiac hypertrophy and LV function at 5 weeks after aortic banding (TAC) in WT and Epac1KO.

(A) Pressure gradients were not different in WT and Epac1KO at 5 weeks after TAC (*n* = 5-12, *P* = NS, *not significant*).

(B-C) LV weight (mg)/tibial length (mm) ratio **(B)** and LV weight (mg)/body weight (BW; g) ratio **(C)** were determined at 5 weeks. The degree of cardiac hypertrophy was increased at 5 weeks, but was similar in WT and Epac1KO (LV/tibial length ratio for WT versus Epac1KO: 7.5 $\pm$ 0.4 versus 7.7 $\pm$ 0.2; LV/BW ratio for WT versus Epac1KO: 4.4 $\pm$ 0.3 versus 4.6 $\pm$ 0.2, *n* = 15, *P* = NS, *not significant*).

(D-E) LVEF was significantly decreased in WT (**P* < 0.01), but not in Epac1KO (*P* = NS, *not significant*) at 5 weeks (WT versus Epac1KO: from 70 $\pm$ 0.8 to 54 $\pm$ 2.0 versus from 60 $\pm$ 1.1 to 61 $\pm$ 0.7%, *n* = 15-31) **(D)**. The data were compared with those from sham-operated controls at 5 weeks in each mouse. Change of LVEF from sham-operated controls at 5 weeks after TAC was significantly greater in WT than that in Epac1KO **(E)** (*n* = 15-31, **P* < 0.01).

(F) LVESD was significantly increased in WT, but not in Epac1KO at 3 weeks after TAC **(C)** (WT versus Epac1KO: from 2.9 $\pm$ 0.04 to 3.3 $\pm$ 0.1 versus from 3.3 $\pm$ 0.1 to

3.2 ± 0.6 mm, *n* = 15-31)

Supplemental Figure 16

LV function and morphological changes in response to long-term ISO infusion or aging in Epac1KO.

(A) Echocardiographic measurements of LV function were performed after long-term ISO infusion (60 mg/kg/day for 1 week) in WT and Epac1KO. LVEF was significantly decreased in WT (**P* < 0.01), but not in Epac1KO (*P* = NS, *not significant*) after long-term ISO infusion (WT versus Epac1KO from 70 ± 0.8 to 60 ± 1.1 versus from 62 ± 1.4 to 60 ± 0.9%, *n* = 14-31)

(B) Representative images of Masson-trichrome-stained sections after long-term ISO infusion in WT and Epac1KO. *Scale bars* : 100 μm

(C) Quantitative analysis of the LV fibrosis area in vehicle and long-term ISO infused heart in both WT and Epac1KO. Cardiac fibrosis was not different between WT and Epac1KO at baseline. It was significantly increased after long-term ISO infusion in WT and Epac1KO, but the magnitude of the increase was much smaller in Epac1KO (WT versus Epac1KO: 4.6 ± 1.6 versus 0.4 ± 0.1%, *n* = 5, **P* < 0.05).

(D) TUNEL-positive myocytes in LV myocardium were counted in WT and Epac1KO and expressed as % of total myocytes. The number of TUNEL-positive myocytes was significantly smaller in Epac1KO than that in WT after long-term ISO infusion (WT versus Epac1KO: 0.27 ± 0.01 versus 0.16 ± 0.02%, *n* = 5, **P* < 0.01).

Comparison of LVEF, LV fibrosis, and TUNEL-positive myocytes in LV apoptosis in old (24-32 months) and young (4-6 months old) Epac1KO and WT

(E) LVEF was significantly decreased in old WT (n = 5), but not in old Epac1KO (n = 6), compared with the values in corresponding young mice (WT: from 70 ± 0.8 to 58 ± 1.3 (*P < 0.01), Epac1KO: from 60 ± 1.1 to 58 ± 2.2%, P = NS, *not significant*).

(F) Quantitative analysis of the area of fibrosis in the heart of old WT and Epac1KO. Cardiac fibrosis was significantly decreased in Epac1KO versus WT (old WT versus old Epac1KO: 3.2 ± 0.2 versus 1.2 ± 0.2%, n = 5-8, *P < 0.01).

(G) TUNEL-positive myocytes in LV myocardium were counted in old WT and Epac1KO and expressed as % of total myocytes. The number of TUNEL-positive myocytes was significantly smaller in Epac1KO than that in WT after chronic ISO infusion for 1 week (old WT versus old Epac1KO: 0.38 ± 0.04 versus 0.22 ± 0.03%, n = 5, *P < 0.05).

Supplemental Figure 17

LV weight (LV; mg)/tibial length (tibia; mm) ratio **(A)** and LV (mg)/body weight (BW; g) ratio **(B)** were determined at 1 week after long-term ISO infusion (60 mg/kg/day). The degree of cardiac hypertrophy was increased at 1 week, but was similar in WT and Epac1KO (LV/tibia for WT versus Epac1KO: 5.7 ± 0.2 versus 5.9 ± 0.2; LV/BW for WT versus Epac1KO: 3.5 ± 0.2 versus 3.7 ± 0.1, n = 14-15).

Supplemental Figure 18

Effect of Epac1 silencing on ISO-mediated neonatal rat cardiac fibroblast proliferation.

(A) ISO-mediated cell proliferations of neonatal rat cardiac fibroblast transfected with control or Epac1 siRNA were examined by MTT assay. They were significantly

increased from baseline after the treatment of ISO (1 or 10 μM) for 24 hours, but the magnitude of the increase were similar (si Control vs. si Epac1: 136 ± 4.6 vs. 140 ± 3.6%, *n* = 8, *P* = NS, *not significant*).

(B) ERK1/2 phosphorylations on threonine 202/tyrosine 204 were significantly increased in cells transfected with control and Epac1 siRNA after t ISO treatment (10 μM for 5 min), but the magnitudes of the increase were similar (si Control versus si Epac1: 151 ± 2.9 versus 154 ± 6.7%, *n* = 4, *P* = NS, *not significant*).

(C) Src phosphorylation on serine-17 were significantly increased in cells transfected with control or Epac1 siRNA after ISO (10 μM) for 30 min, but the magnitudes of the increase were similar (si Control vs. si Epac1: 233 ± 12 versus 235 ± 13%, *P* = NS, *not significant*, *n* = 7-8,).

(D) Representative immunoblotting results. T-ERK, total ERK1/2; p-ERK, phosphorylated ERK1/2, T-Src, total Src; p-Src, phosphorylated Src.

Supplemental Figure 19

(B-C) Incidence of spontaneous activity (SA) in the pulmonary vein was not different in WT (4/17:24%) and Epac1KO (7/24:29%) at baseline (*P* = NS, *not significant*) **(B)**. However, it was increased after noradrenaline (1 μM) treatment in both WT and Epac1KO, but the magnitudes of the increase were significantly smaller in Epac1KO

(12/17:71%) than that in WT (15/15:100%) (*$P < 0.05$ Fisher exact probability test) **(C)** *Inserts*; representative tracing results of spontaneous activity in the pulmonary vein prepared from WT **(upper)** and Epac1KO **(lower)** are shown **(A)**.

Supplemental Figure 20

Generation of Epac2KO

(A) Targeted disruption of the Epac2 gene is shown. The partial structure of the Epac2 (WT) and the resultant mutant allele (Epac2KO) are shown. The positions of the phosphoglycerate kinase promoter neo cassette (Pr-Neo-pA), 5'-probe and 3'-probe are indicated.

(B) Southern blot analysis of targeted embryonic stem cell (ES) clones is shown. Genomic DNA from control TT2 ES cells and homologous targeted clones were digested with AvrII and hybridized with the probe as indicated in A.

(C) Genotyping of mice by PCR.

(D) Northern blot analysis of Epac1, Epac2, and glyceraldehyde dehydrogenase (GAPDH) in the heart of WT and Epac2KO mice is shown.

Supplemental Figure 21

(A) Phosphorylation on serine-16 (Ser-16) was similar between WT and Epac2KO at baseline (WT versus Epac1KO: 100 $\pm$ 20 versus 104 $\pm$ 20%, n = 9-14, P = NS, *not significant*). The ratio of phosphorylated/total protein expression of phospholamban in WT was taken as 100% in each determination. Representative immunoblotting results of phosphorylation of phospholamban on serine-16. T-PLN, total phospholamban; p-PLN, phosphorylated phospholamban.

(B) Phosphorylation on threonine-17 (Thr-17) was similar between WT and Epac2KO at baseline (WT versus Epac2KO: 100 ± 13 versus 92 ± 12%, *n* = 6-8, *P* = NS, *not significant*). The ratio of phosphorylated/total protein expression of PLN in WT was taken as 100% in each determination. Representative immunoblotting results of phosphorylation of PLN on serine-16. T-PLN, total phospholamban; p-PLN, phosphorylated phospholamban.

Supplemental Figure 22

Changes in cardiac hypertrophy and LV function at 3 weeks after aortic banding in WT and Epac2KO. Echocardiographic measurements of LV function were performed at 3 weeks after TAC of WT and Epac2KO and in sham-operated controls (Sham).

Comparison of cardiac hypertrophy after aortic banding in WT and Epac2KO.

(A) LV weight (mg)/tibial length (mm) ratio were determined at 3 weeks. The degree of cardiac hypertrophy was increased at 3 weeks, but was similar in WT and Epac2KO (LV/tibial length ratio for WT versus Epac2KO: 7.1 ± 0.4 versus 6.8 ± 0.2, *n* = 4, *P* = NS, *not significant*).

(B) LVEF was significantly decreased in both WT and Epac2KO at 3 weeks (WT (WT versus Epac2KO: from 73 ± 1.1 to 55 ± 3.1 versus from 72 ± 1.1 to 58 ± 5.2%, $P < 0.05$, *n* = 4-5), but the magnitudes of the decrease were similar (*P* = NS, *not significant*).

(C) LVESD was increased similarly in WT and Epac2KO at 3 weeks after banding (WT versus Epac2KO: from 2.7 ± 0.07 to 3.1 ± 0.2 versus from 2.6 ± 0.05 to 3.1 ± 0.2 mm, $P < 0.05$, *n* = 4-13), but the magnitudes of the increase were similar (*P* = NS, *not significant*).

(D) Representative gross LV section of Masson-trichrome staining in sham-operated and TAC-operated WT and Epac2KO heart. Note that the degree of cardiac hypertrophy and the fibrotic area after aortic banding were similar.

(E) There was no difference in the degree of fibrosis between WT and Epac2KO at baseline. Thus, the development of cardiac fibrosis was unaffected in Epac2KO (WT versus Epac2KO: 0.4 $\pm$ 0.08 versus 0.4 $\pm$ 0.09%, *P* = NS, *not significant*, *n* = 5). Aortic banding increased the area of fibrosis in both WT and Epac2KO, but the magnitudes of increase were similar (WT versus Epac2KO: 22 $\pm$ 3.6 versus 18 $\pm$ 5.3%, *P* = NS, *not significant*, *n* = 4).

(F) TUNEL-positive myocytes in LV myocardium were counted in WT and Epac2KO and expressed as % of total myocytes. The number of TUNEL-positive myocytes was not different in WT and Epac2KO at baseline (WT versus Epac1KO: 0.09 $\pm$ 0.02 versus 0.09 $\pm$ 0.01%, *n* = 5, *P* = NS, *not significant*) and the magnitudes of the increase after TAC were similar (WT versus Epac1KO: 0.8 $\pm$ 0.04 versus 0.8 $\pm$ 0.05%, *n* = 4-5, *P* = NS, *not significant*).

Supplemental Table 1

Heart Size and Cardiac Function in Epac2KO

	WT (*n*)	Epac2KO (*n*)
Age, month	4.7 ± 0.3 (20)	4.6 ± 0.2 (17)
BW, g	30 ± 0.5 (6)	25 ± 0.7 (9) *
Tibia, mm	17.5 ± 0.1 (10)	17.3 ± 0.1 (10)
LV/tibia (mg/mm)	5.7 ± 0.1 (5)	5.2 ± 0.2 (7)
LV/BW (mg/g)	3.7 ± 0.04 (5)	3.5 ± 0.1 (8)
LVEDD, mm	4.3 ± 0.1 (10)	4.1 ± 0.1 (8)
LVESD, mm	2.9 ± 0.1(10)	2.8 ± 0.1 (8)
LVEF, %	70 ± 1.4 (10)	68 ± 2.3 (8)
%FS	34 ± 1.1 (10)	32 ± 1.5 (8)
Max dP/dt, mmHg	9166 ± 611 (10)	9202 ± 453 (9)
Min dP/dt, mmHg	–9334 ± 324 (9)	–9495 ± 657 (9)

Data are mean ± SEM

LVEF: Left ventricular ejection fraction

LVEDD: Left ventricular end-diastolic diameter

LVESD: Left ventricular end-systolic diameter

%FS: % fractional shortening

*$P < 0.01$

Supplemental Figure 1

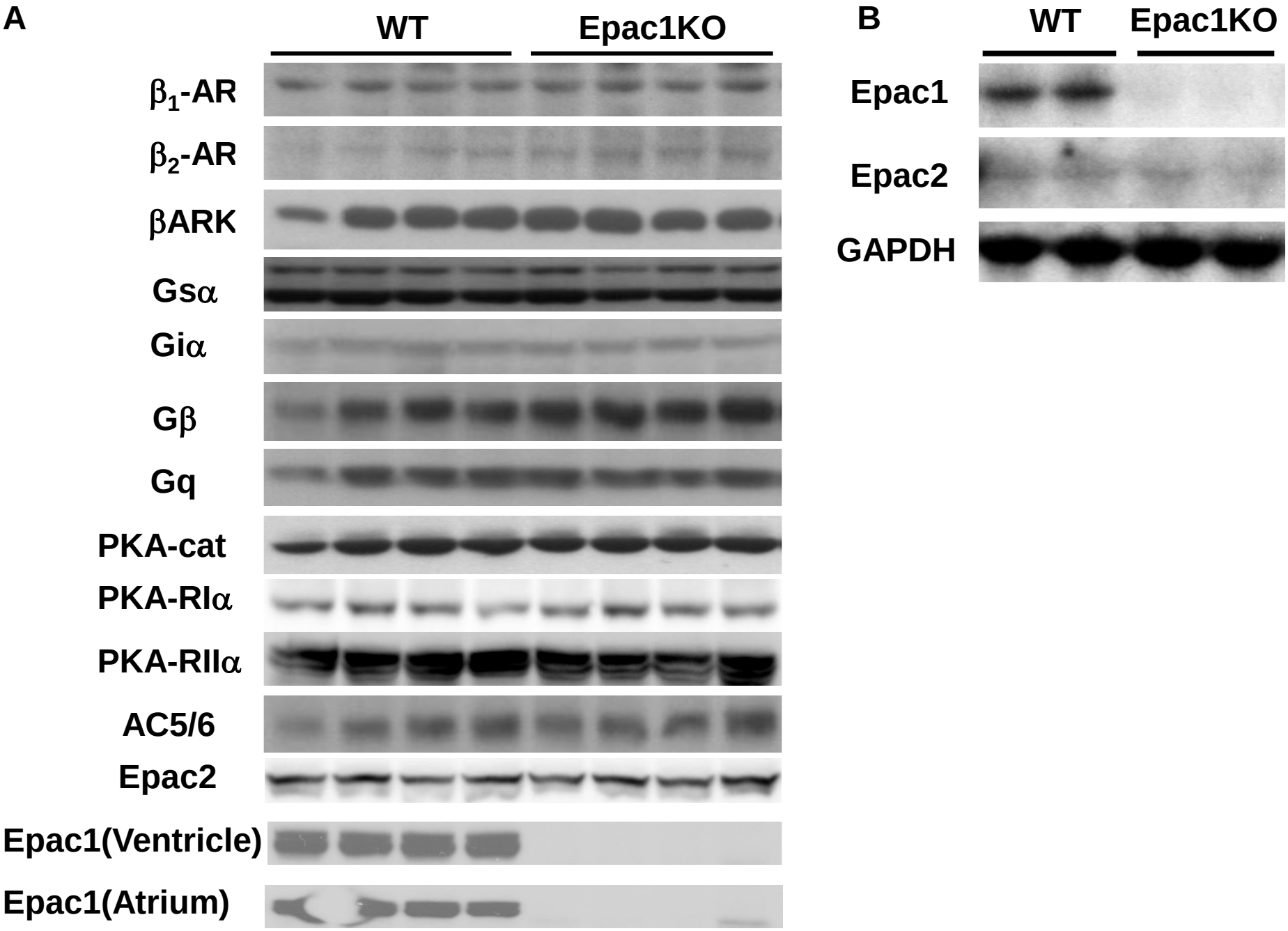

Supplemental Figure 2

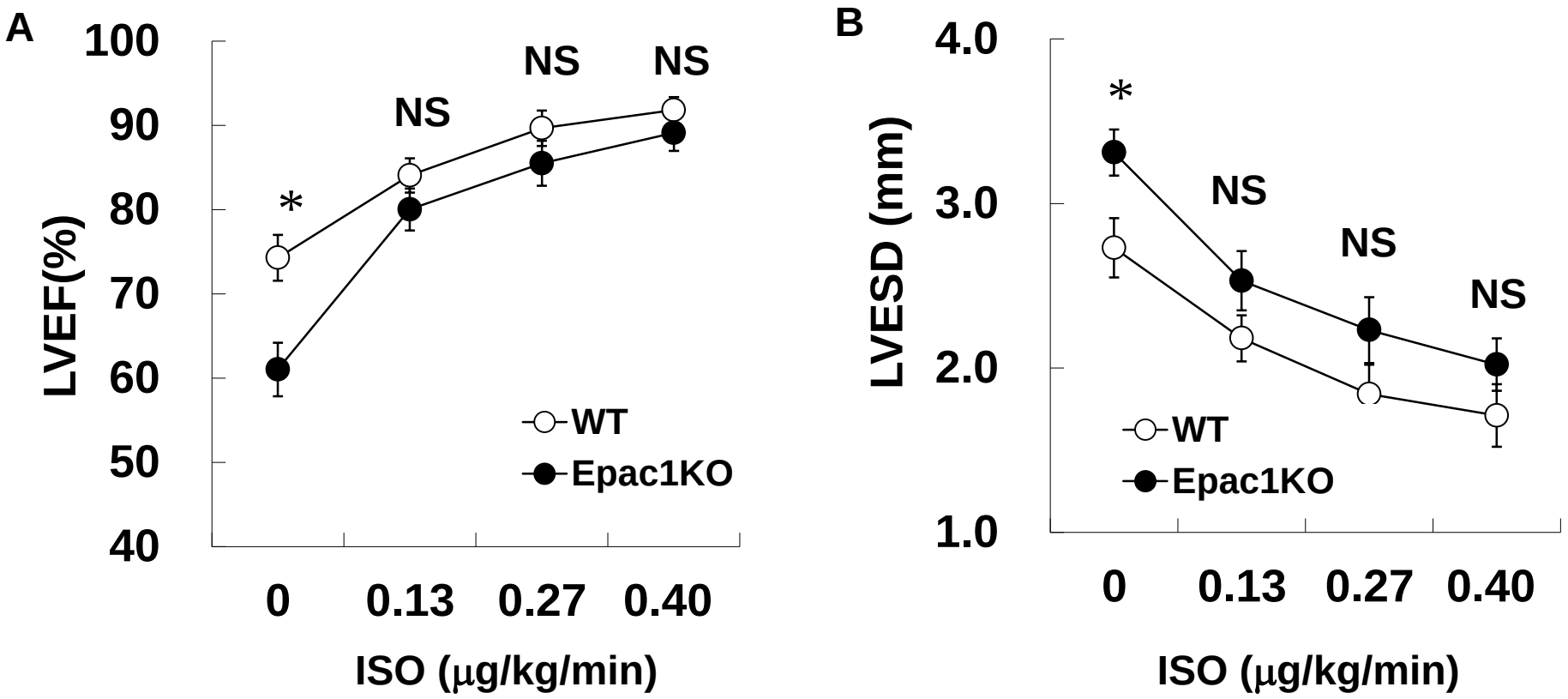

Supplemental Figure 3

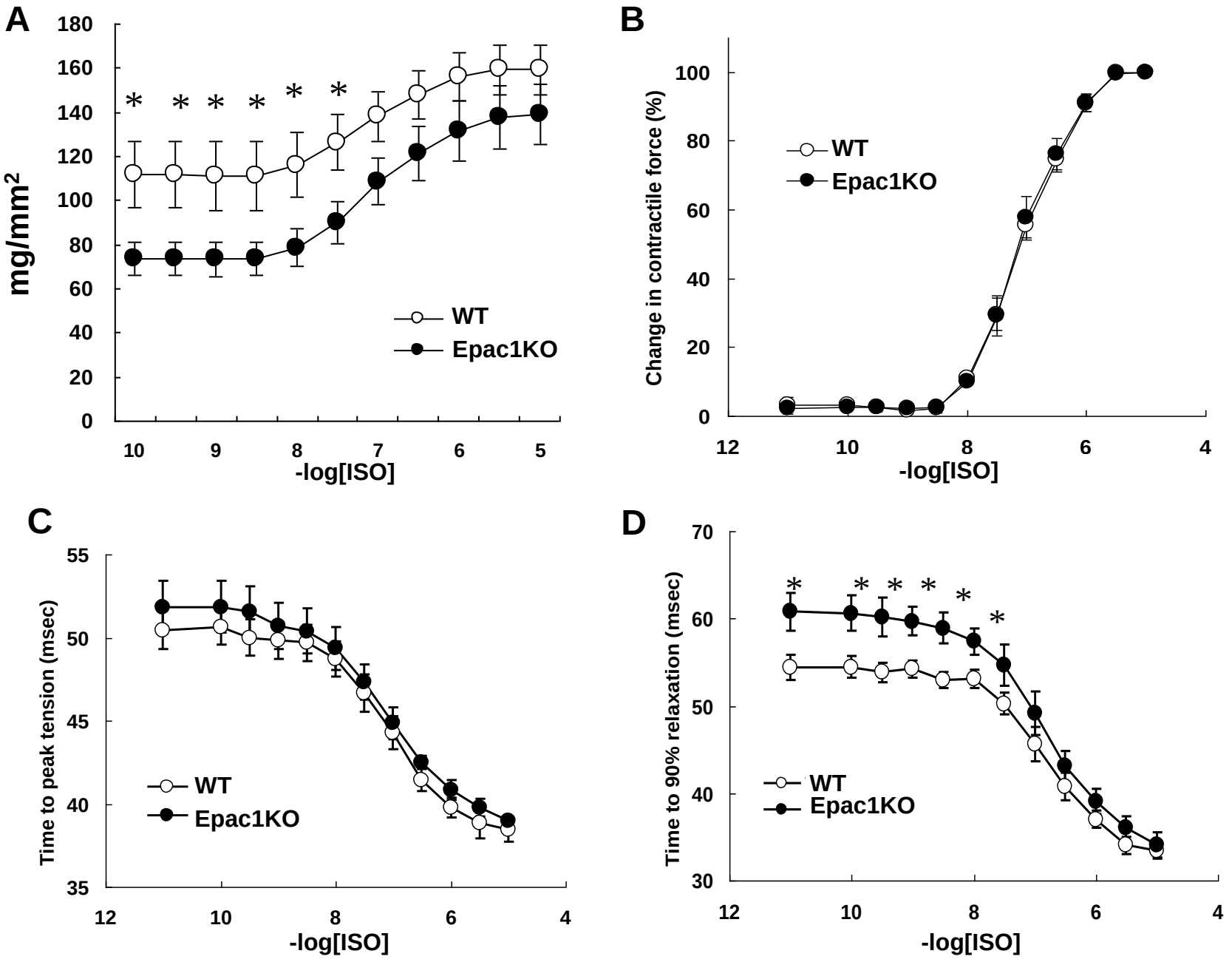

Supplemental Figure 4

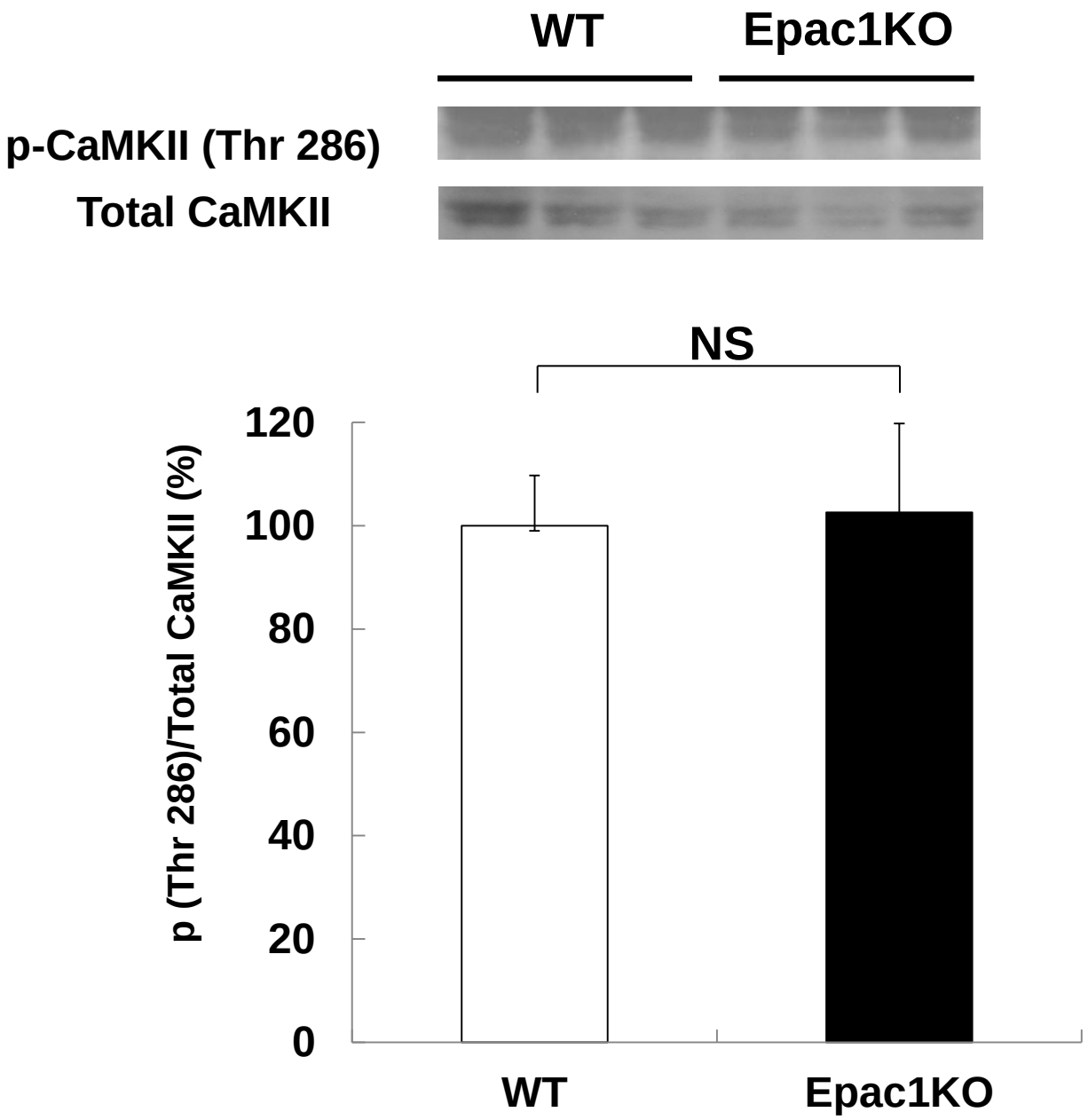

Supplemental Figure 5

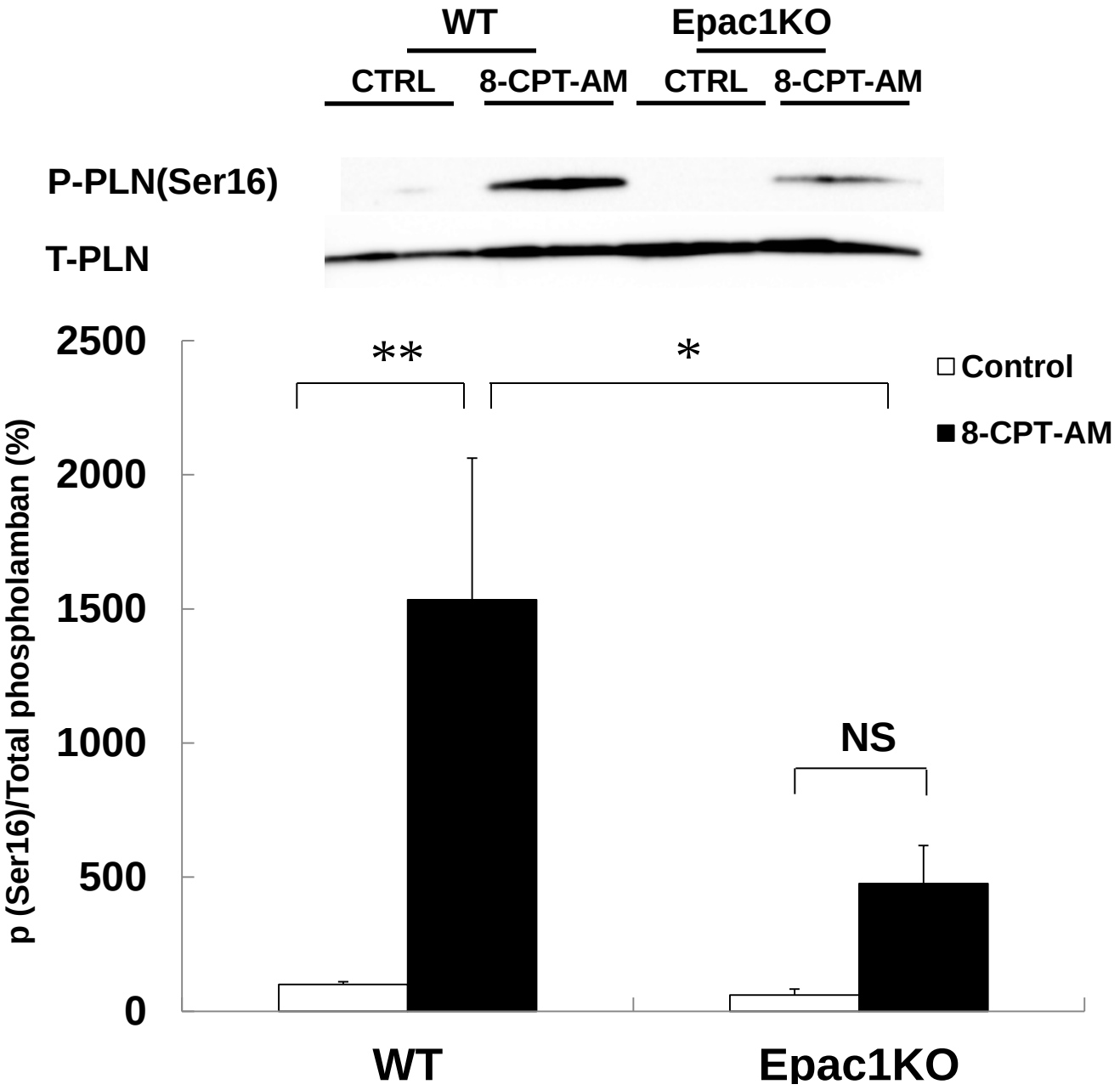

Supplemental Figure 6

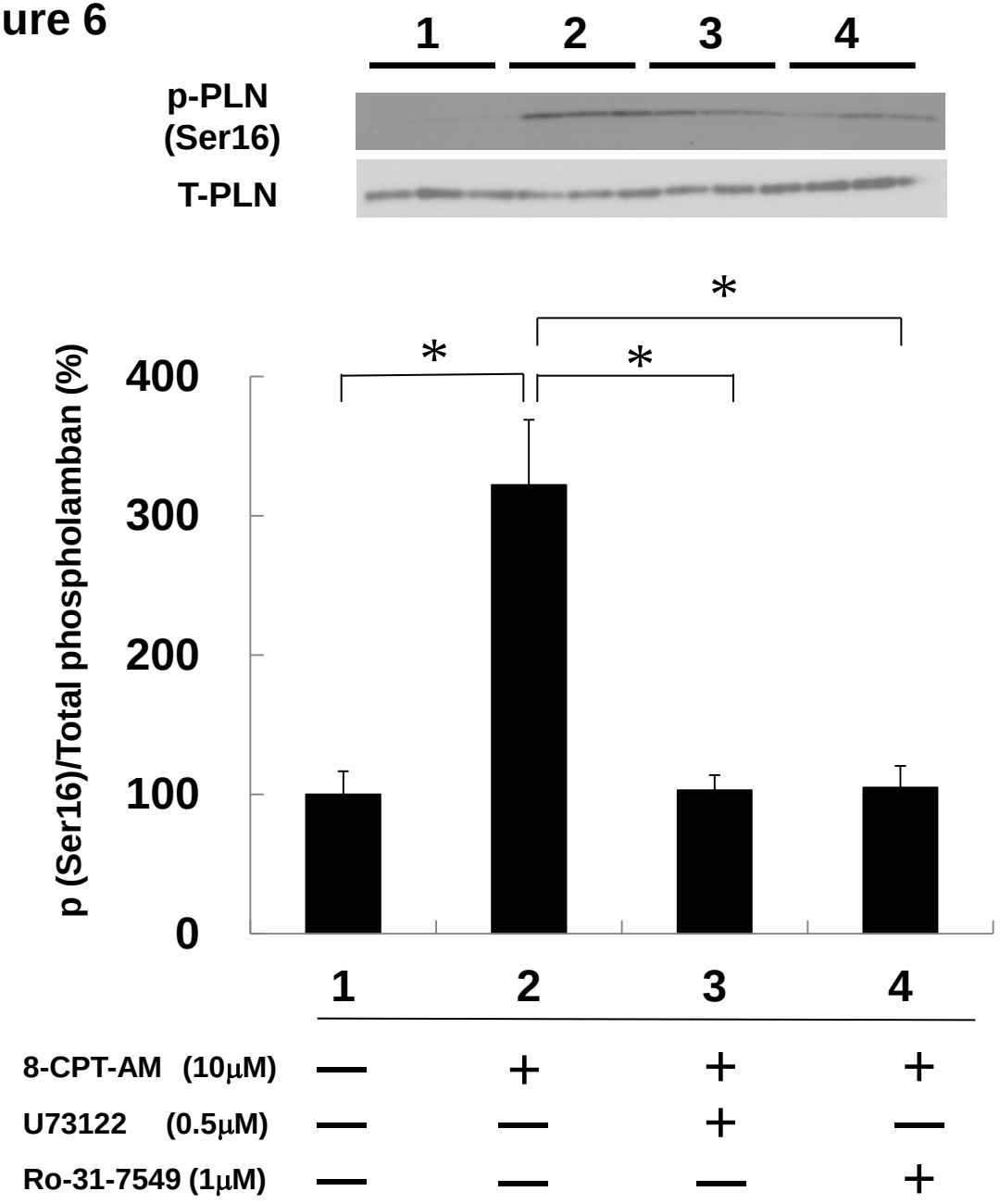

Supplemental Figure 7

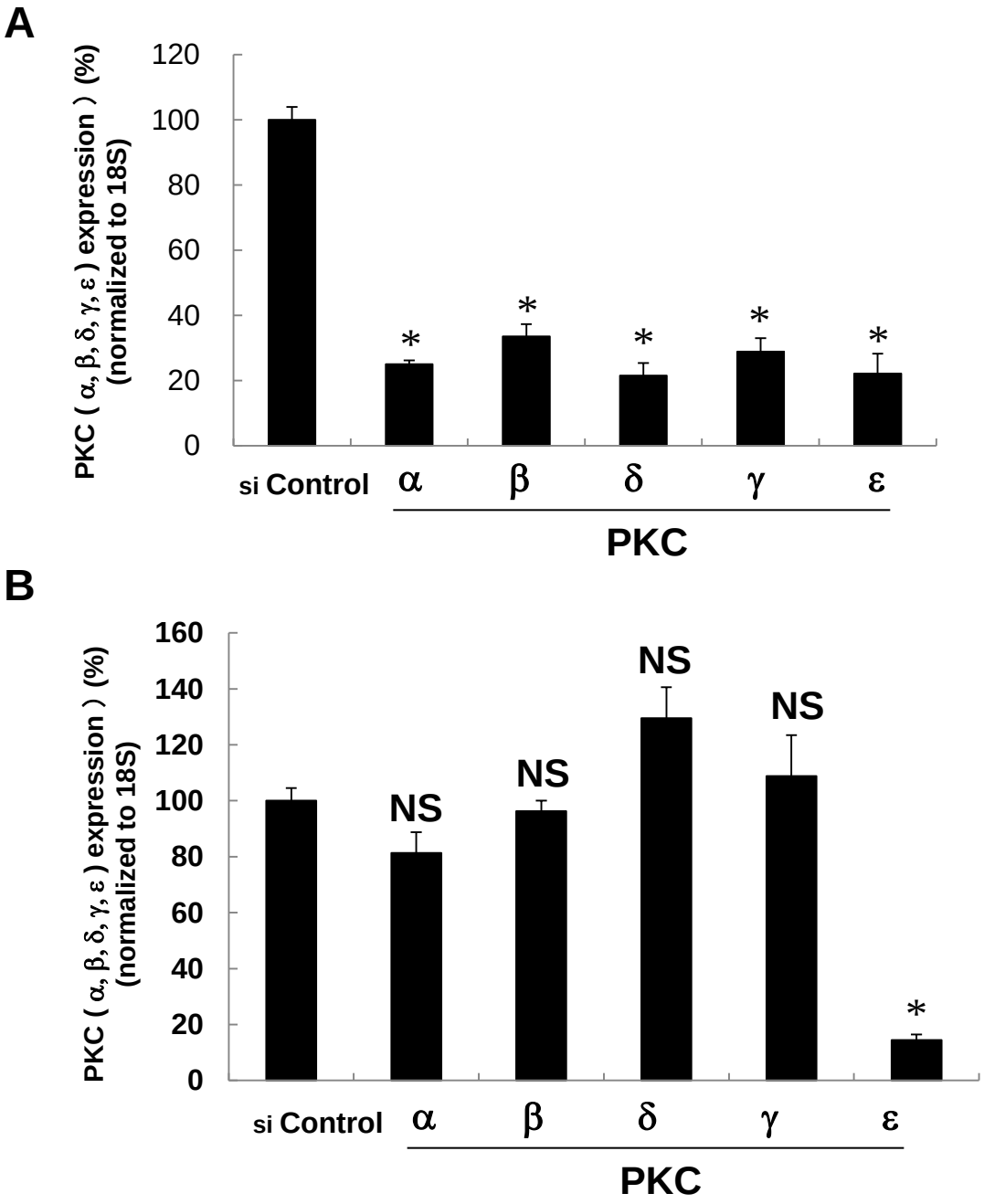

Supplemental Figure 8

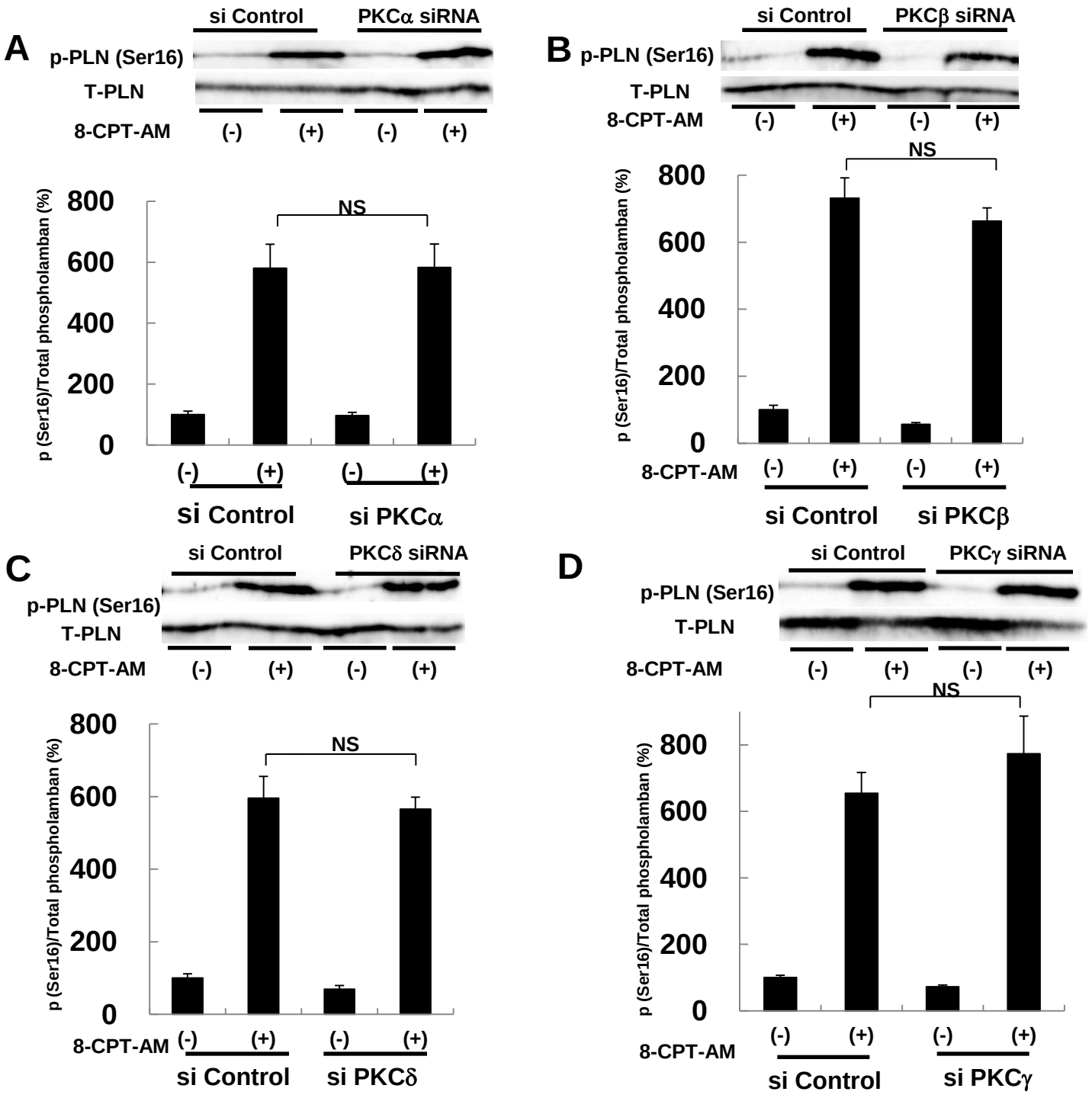

Supplemental Figure 9

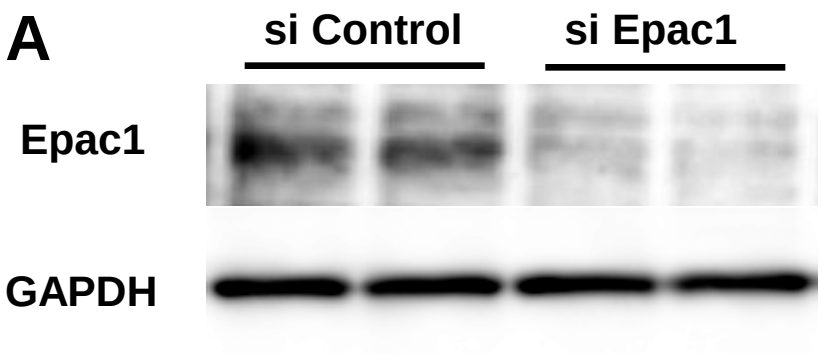

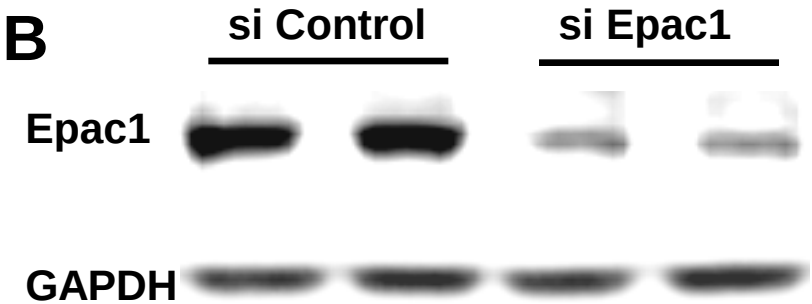

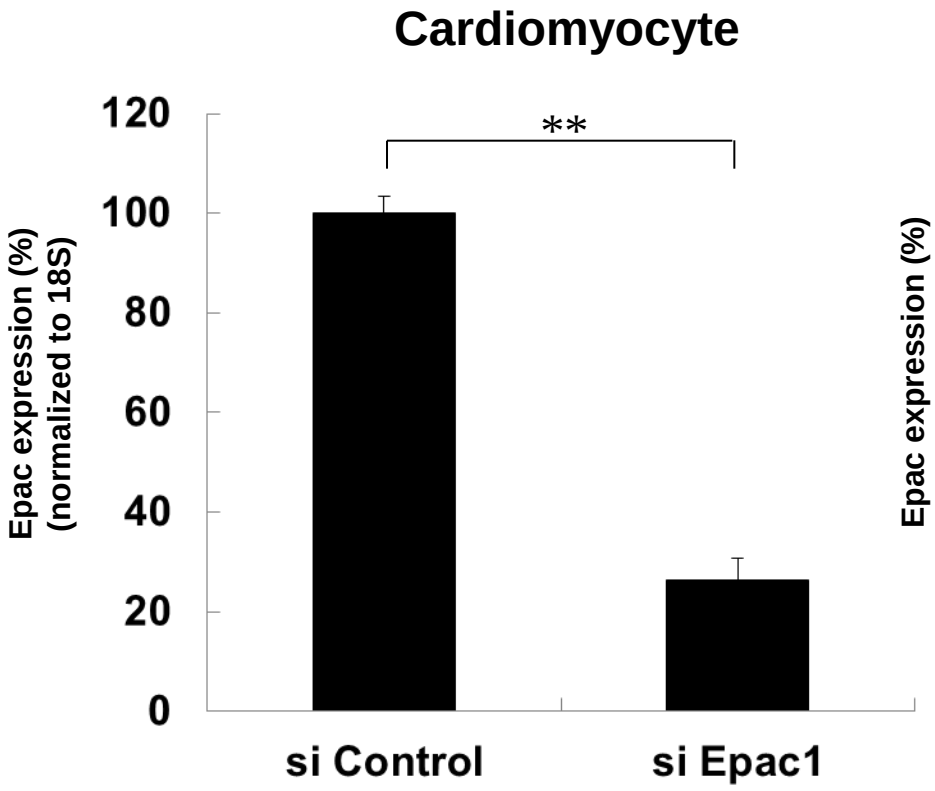

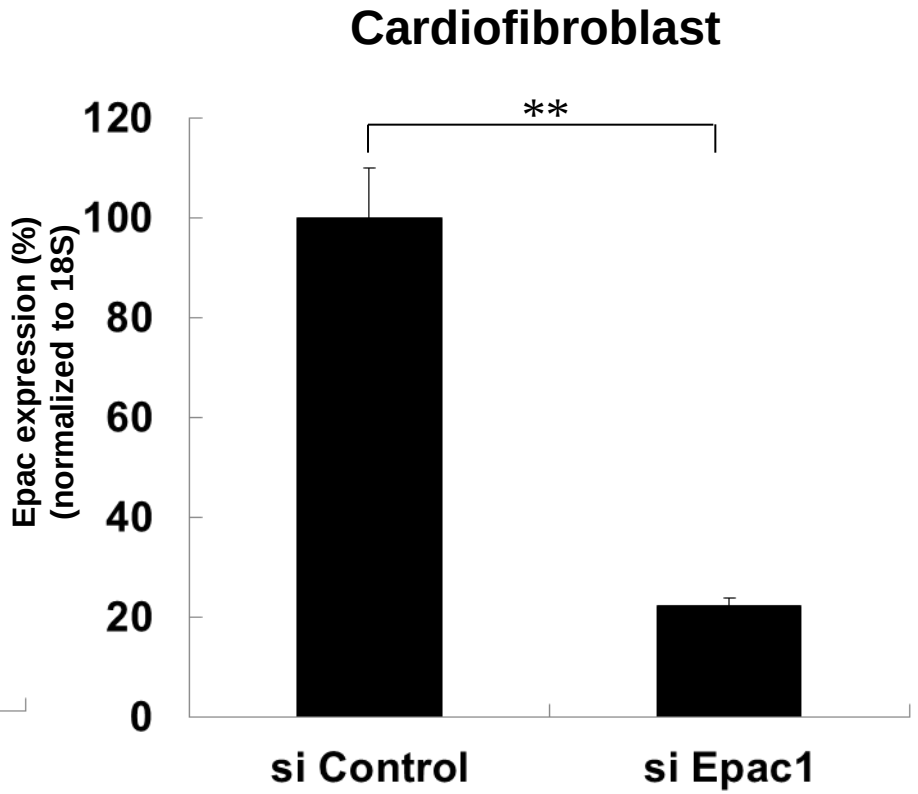

Supplemental Figure 10

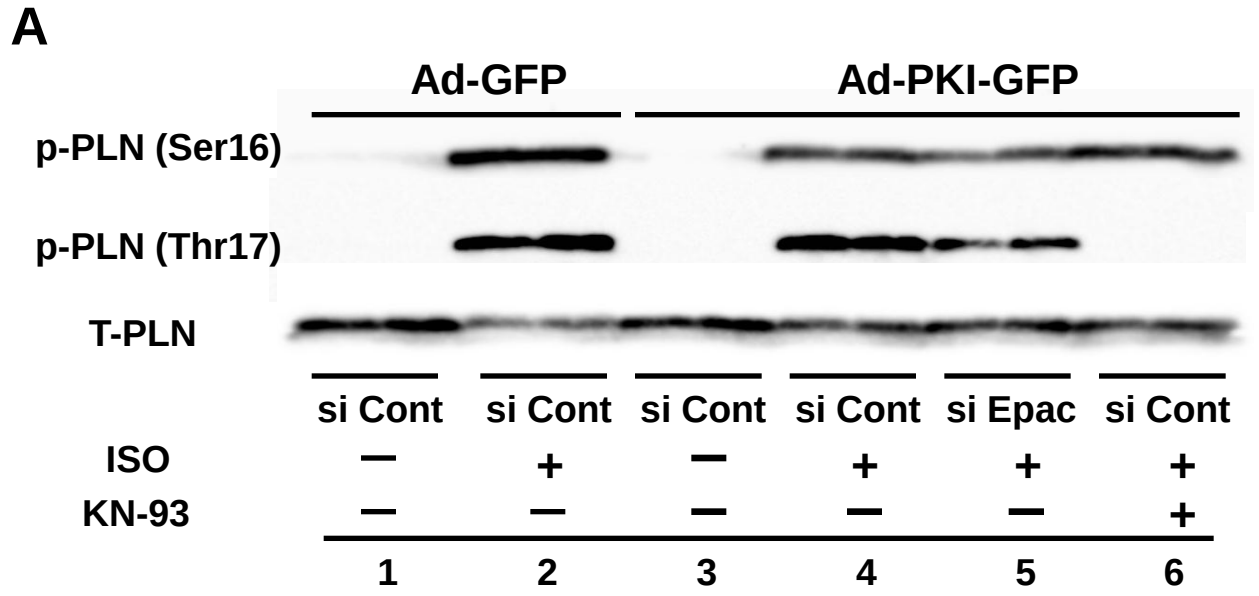

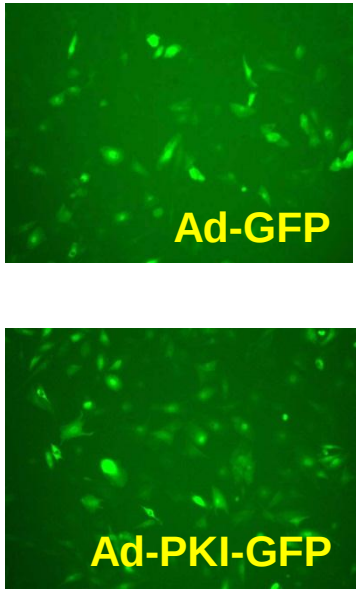

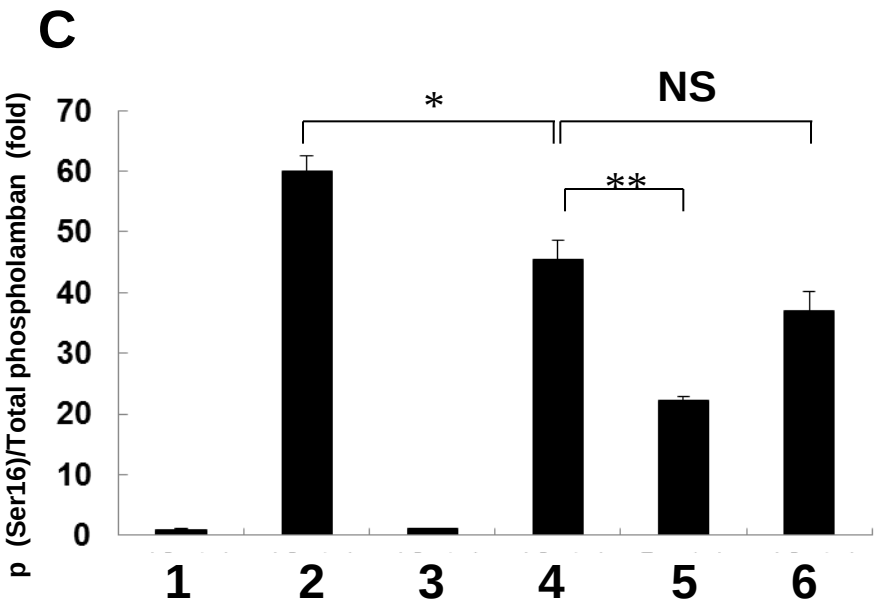

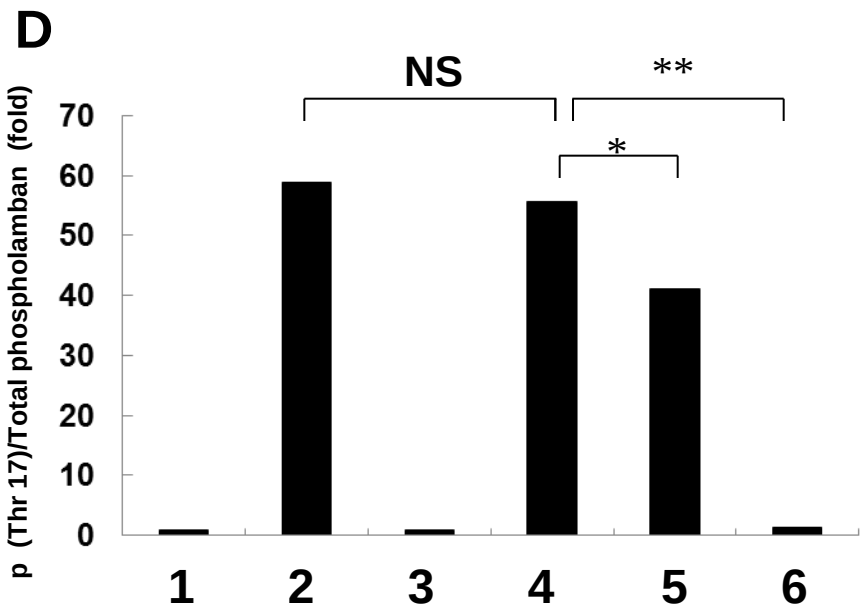

Supplemental Figure 11

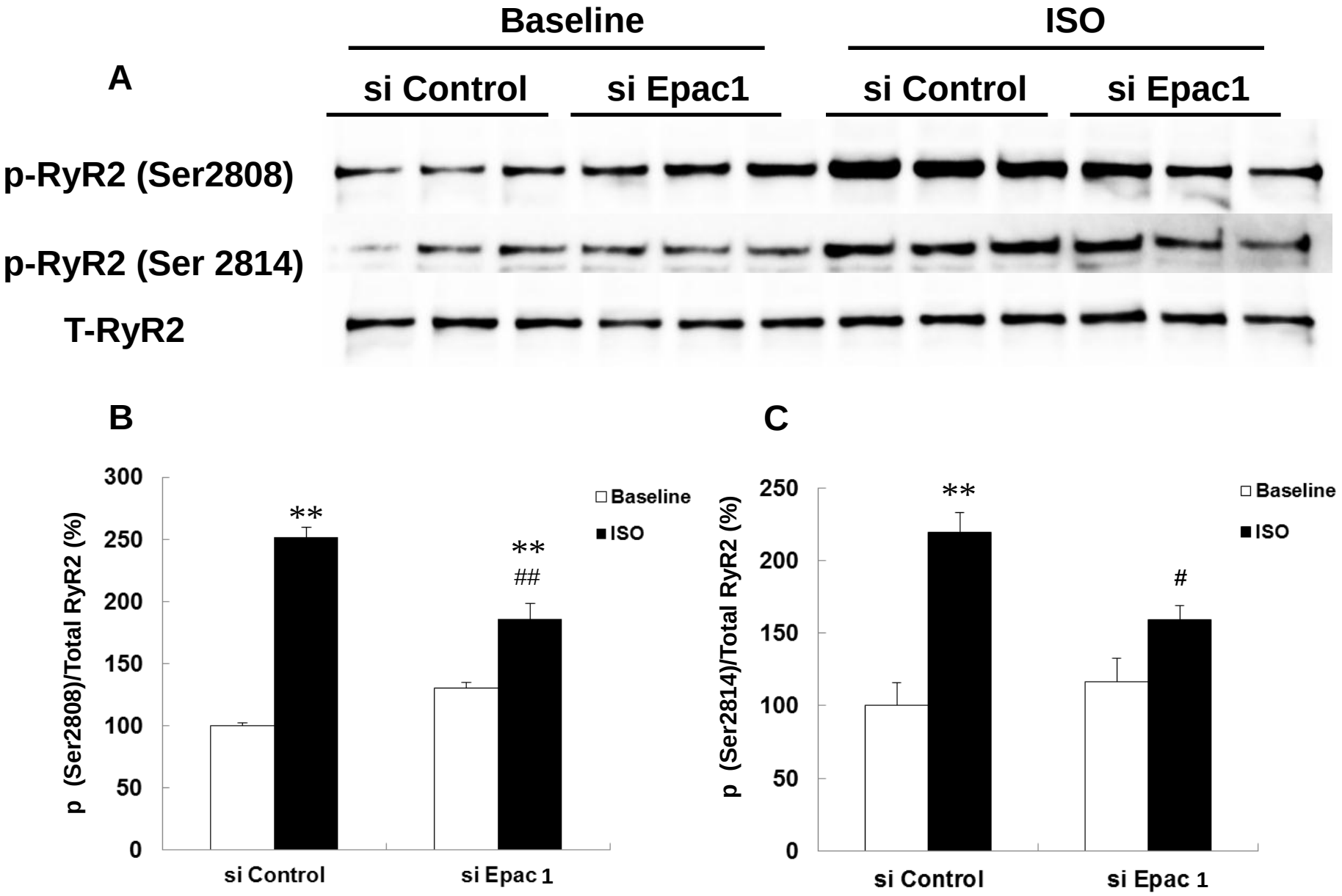

Supplemental Figure 12

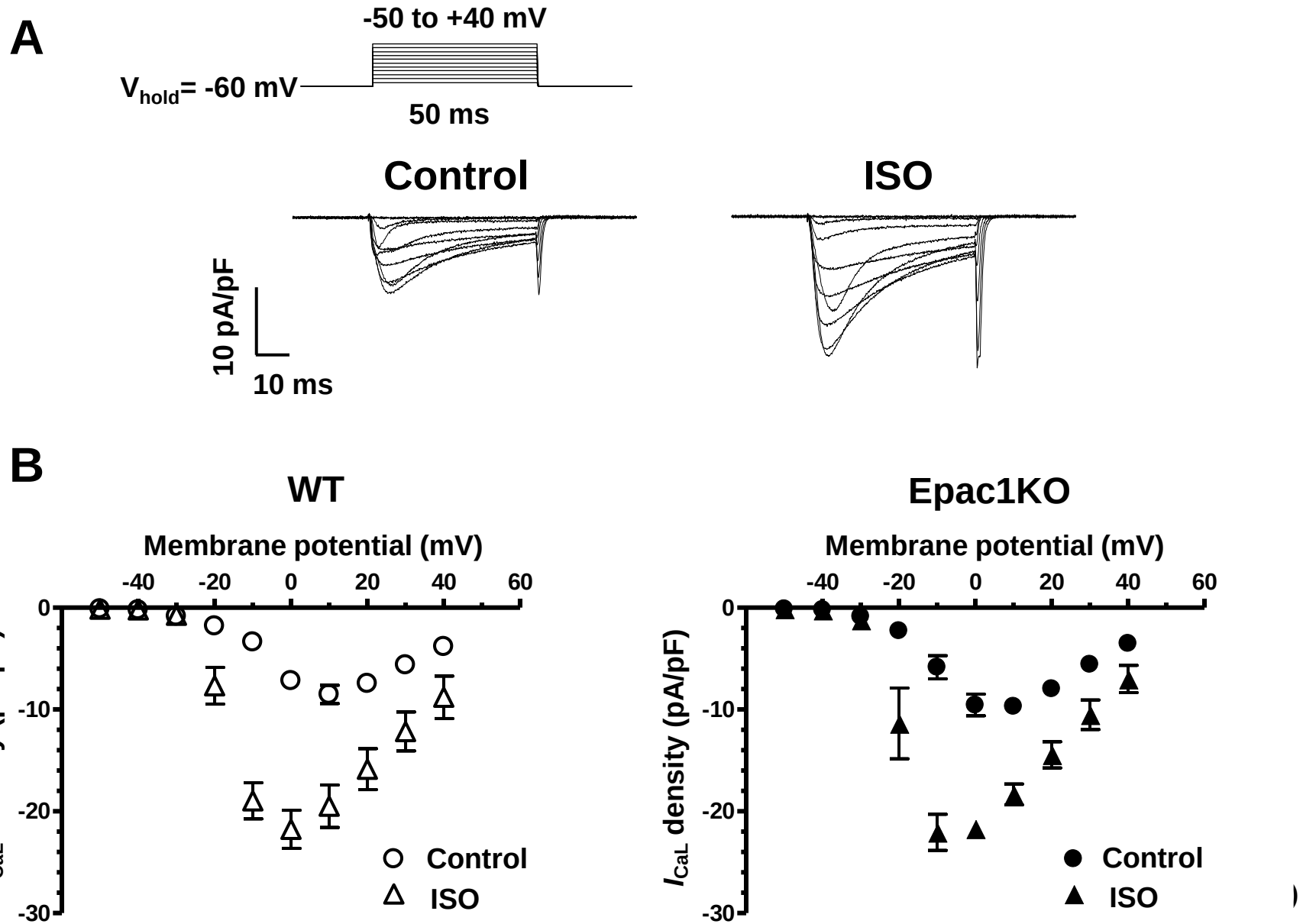

Supplemental Figure 13

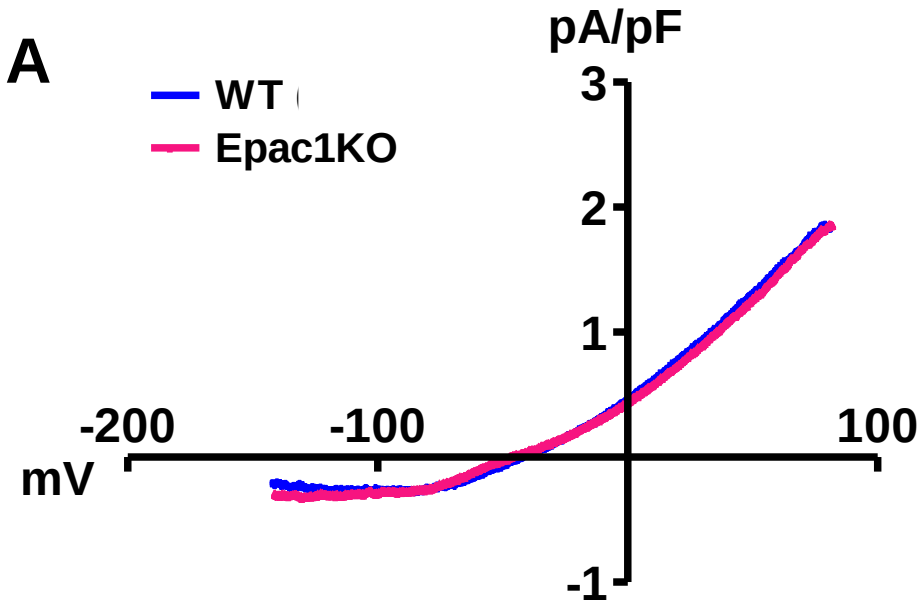

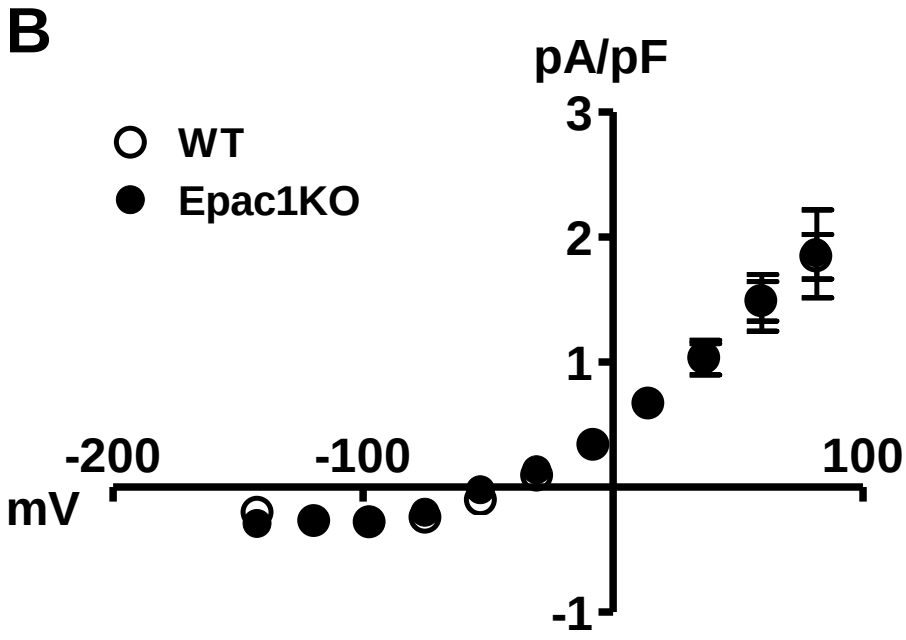

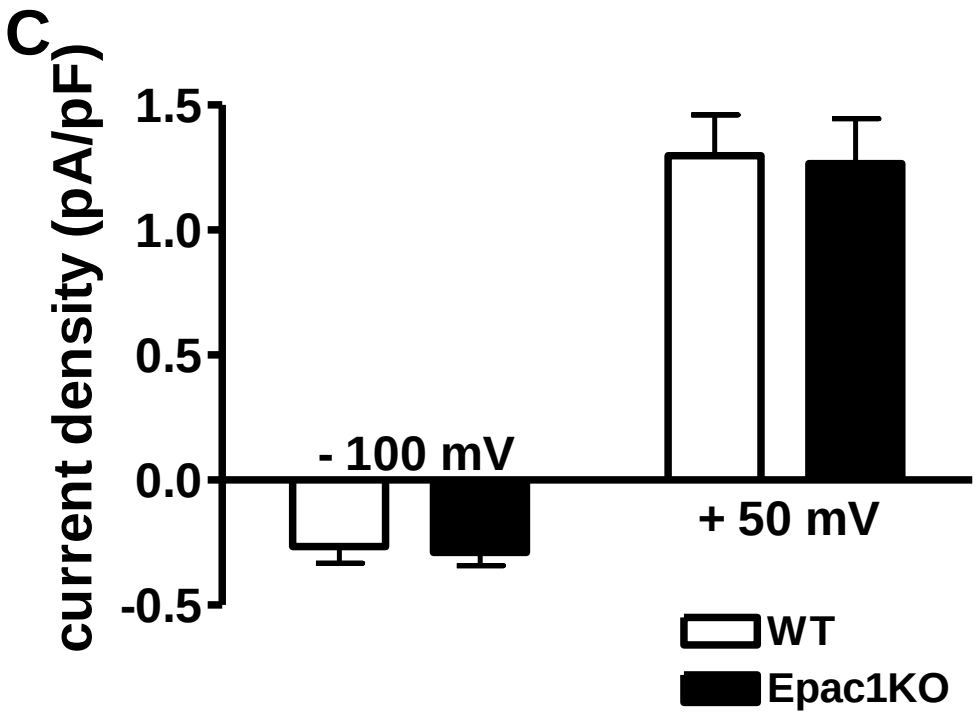

Supplemental Figure 14

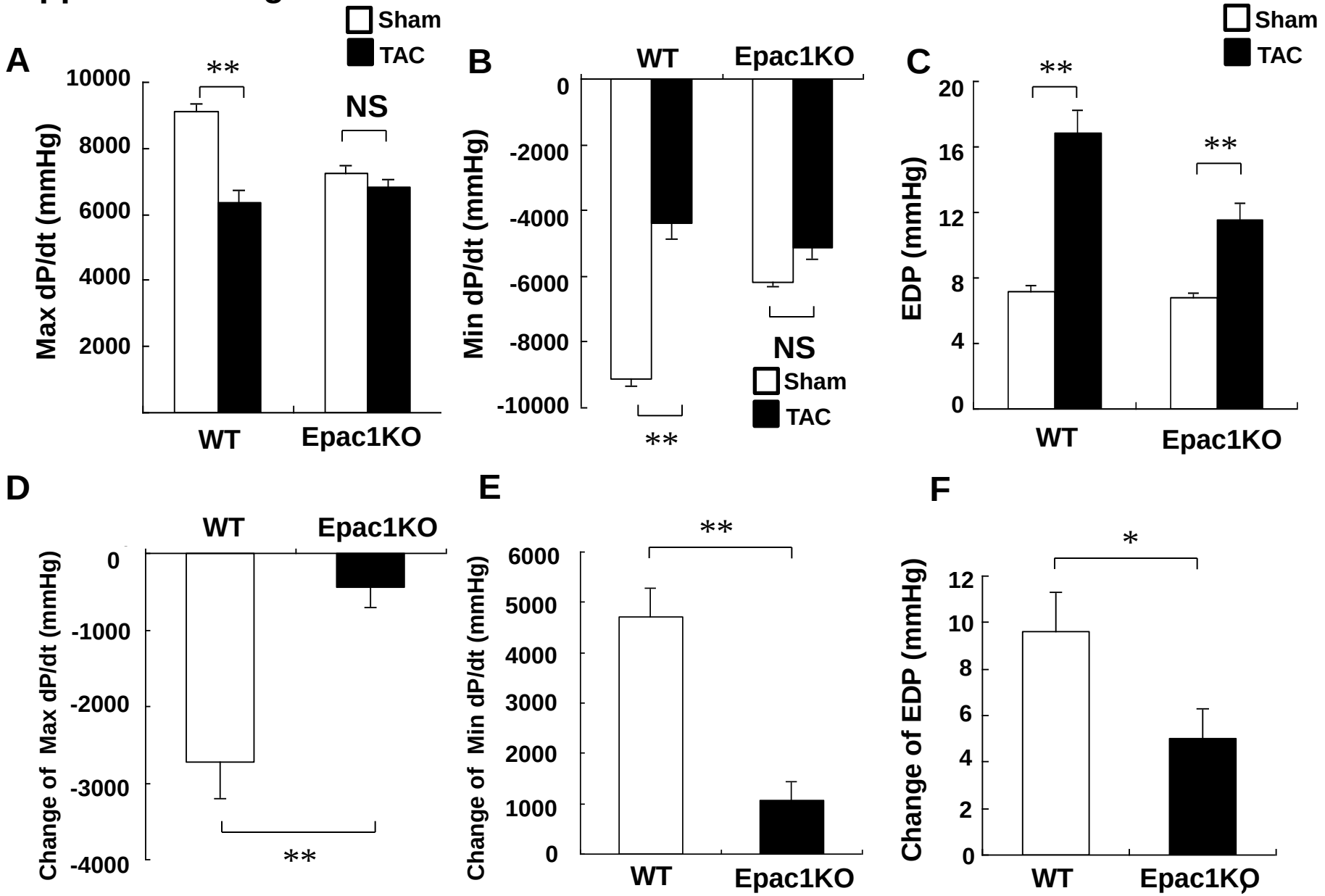

Supplemental Figure 15

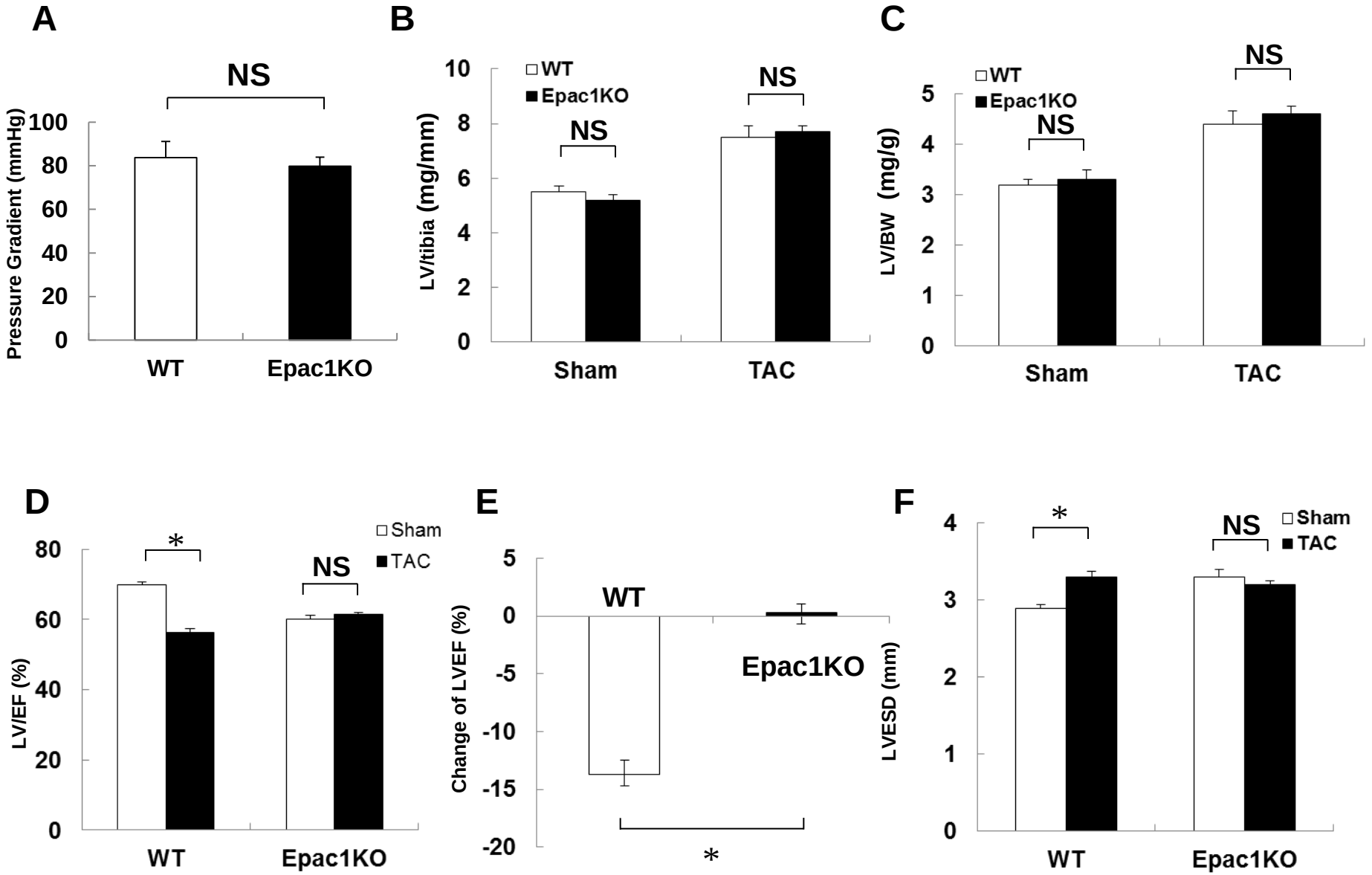

Supplemental Figure 16

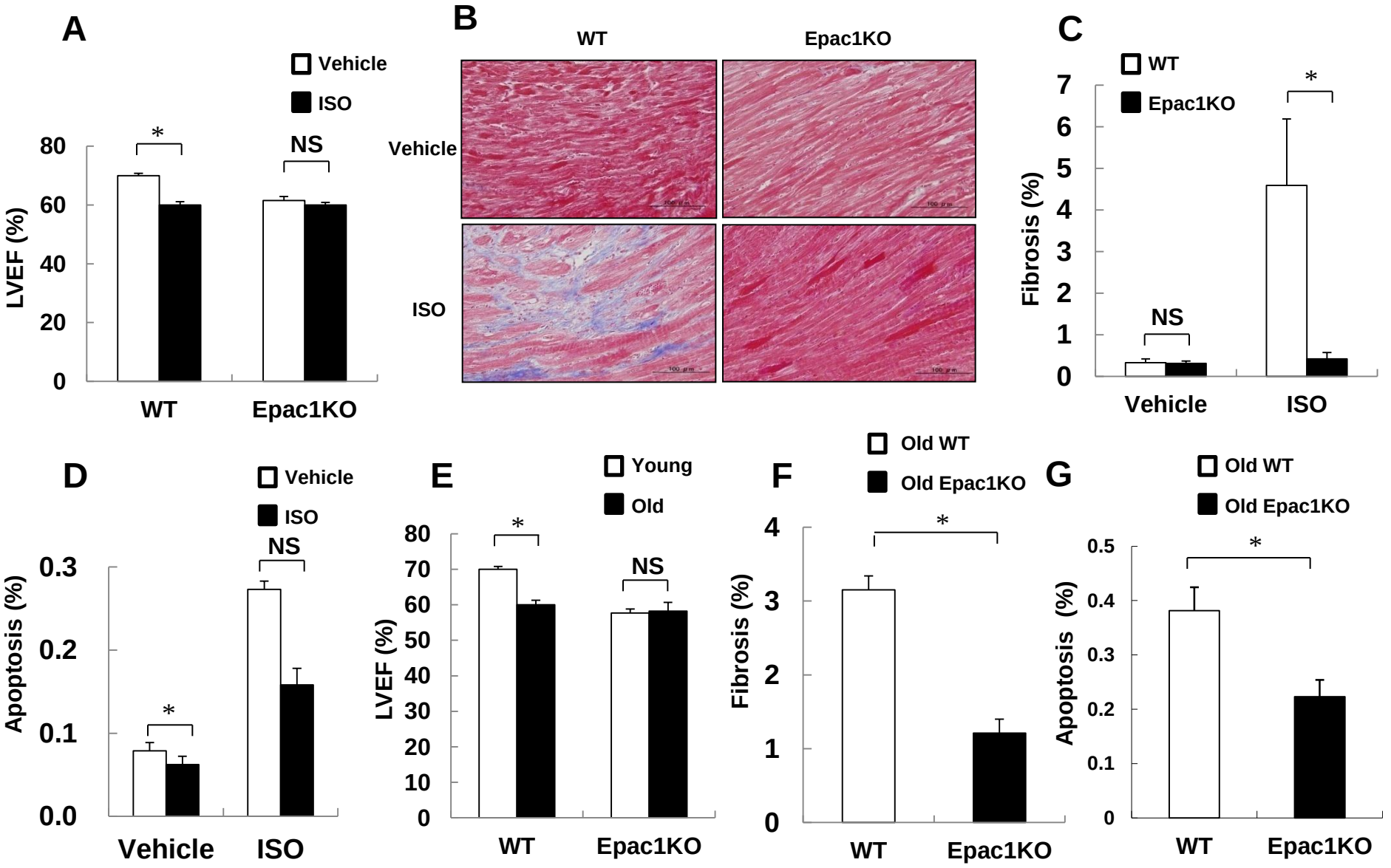

Supplemental Figure 17

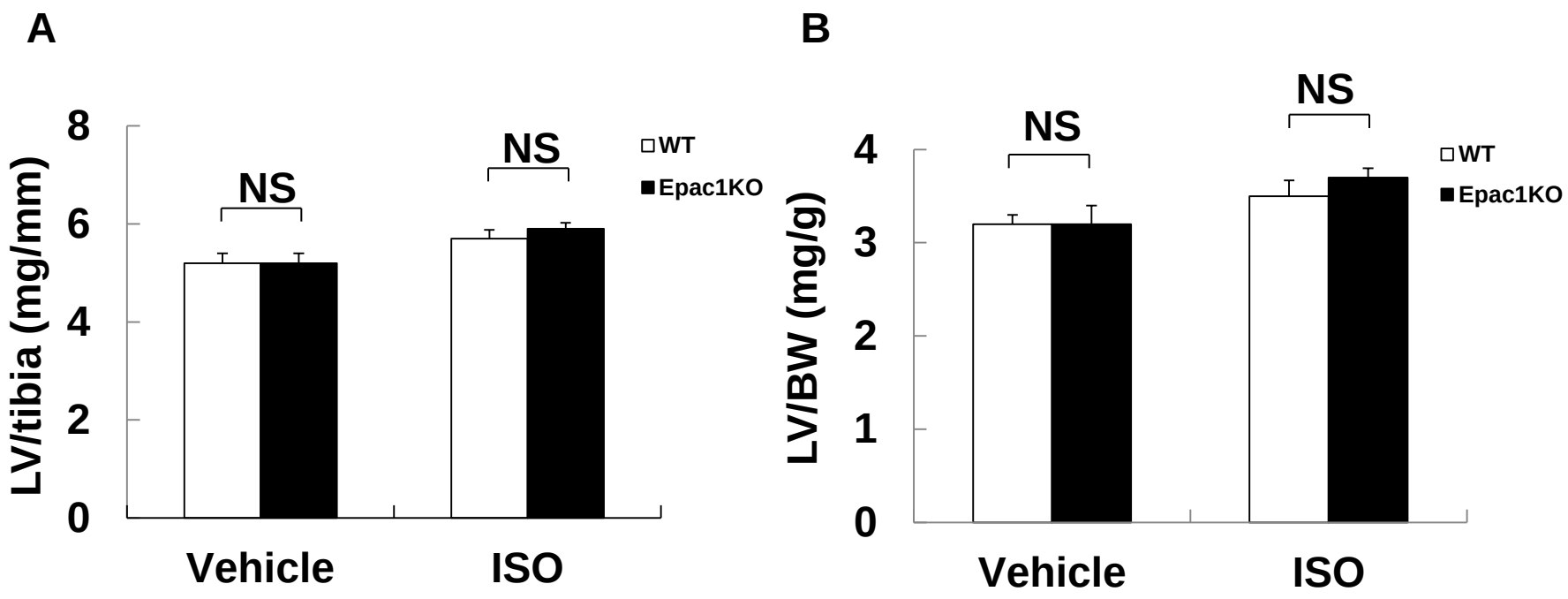

Supplemental Figure 18

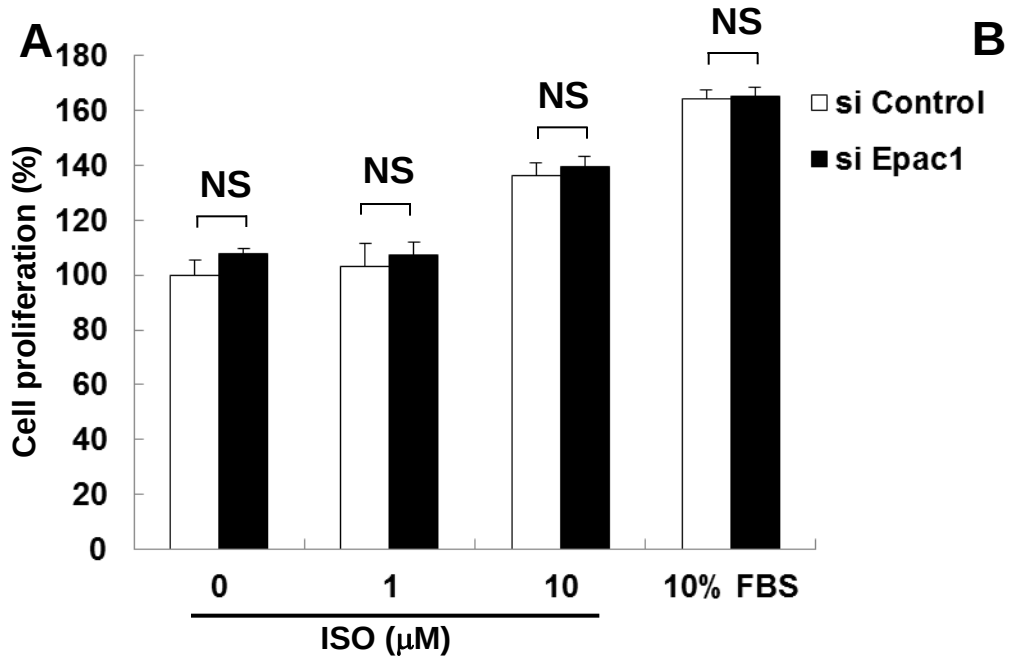

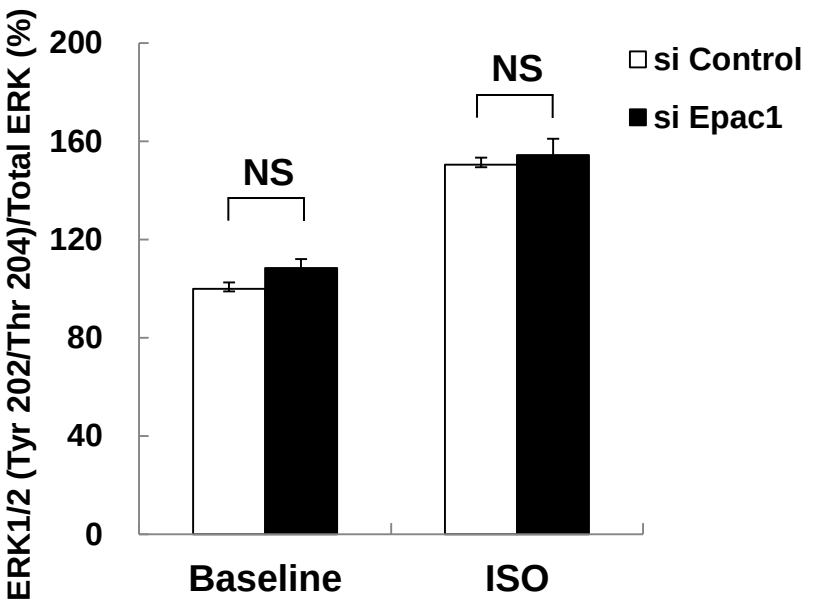

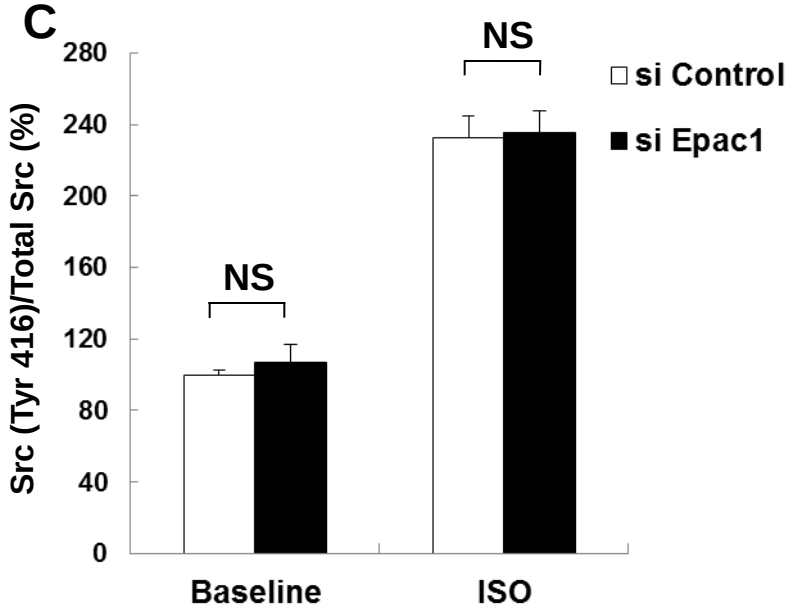

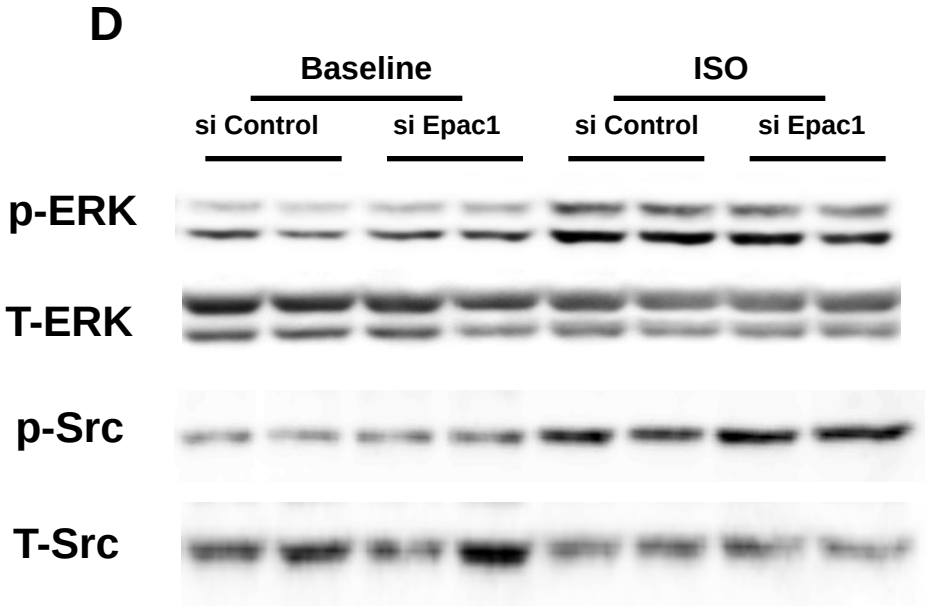

Supplemental Figure 19

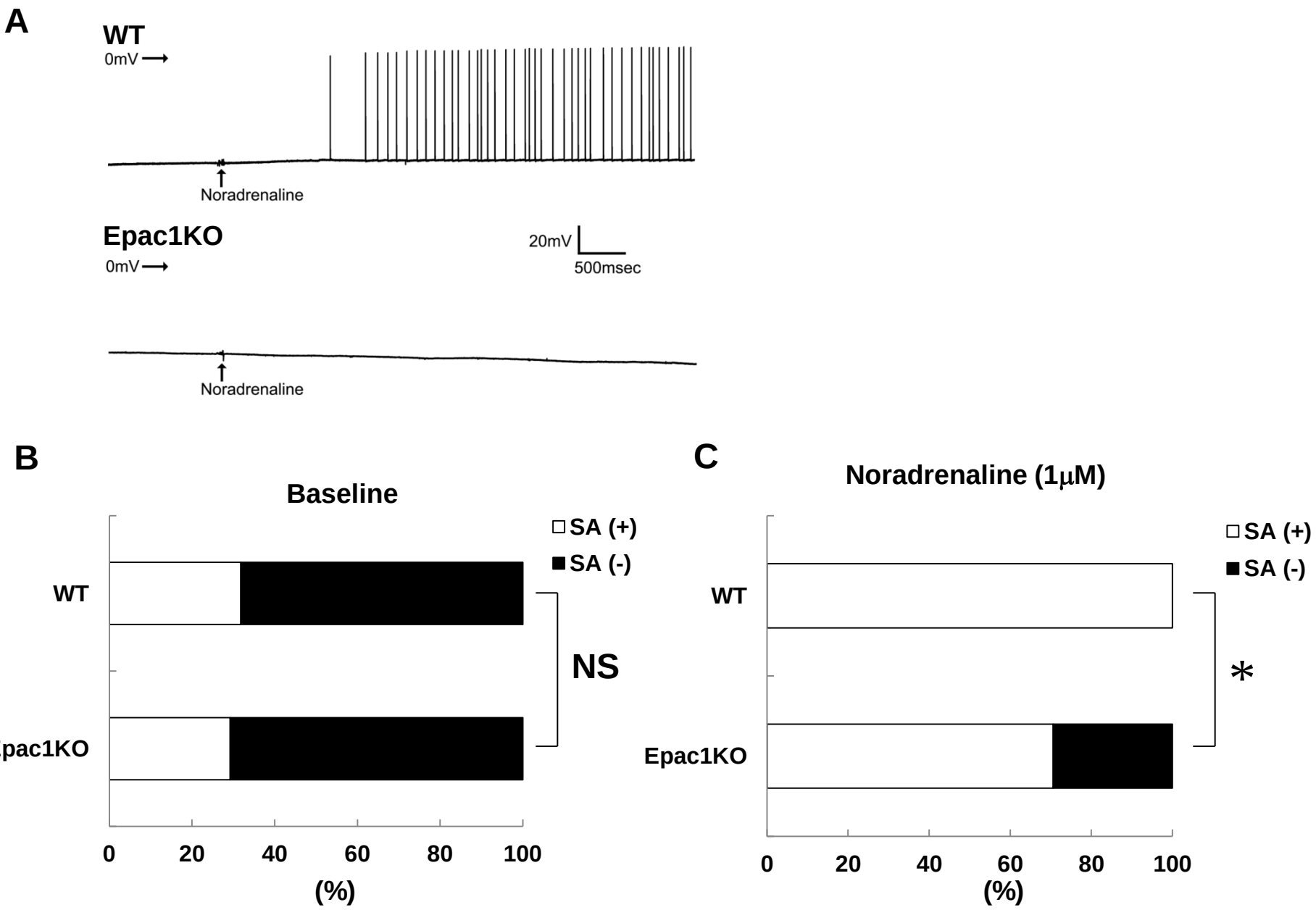

Supplemental Figure 20

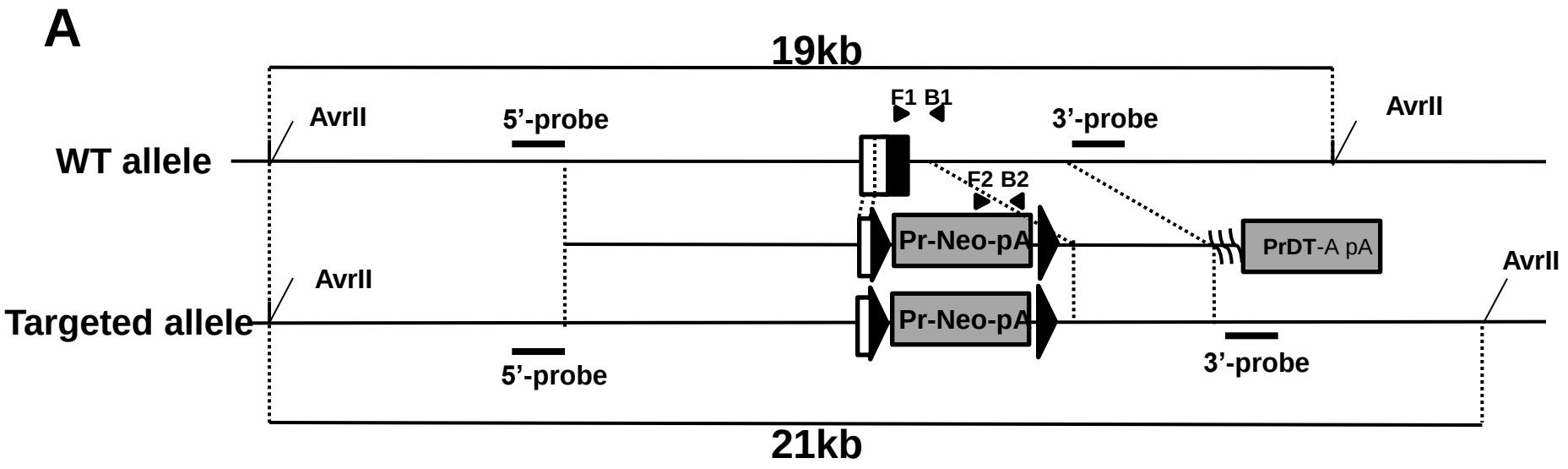

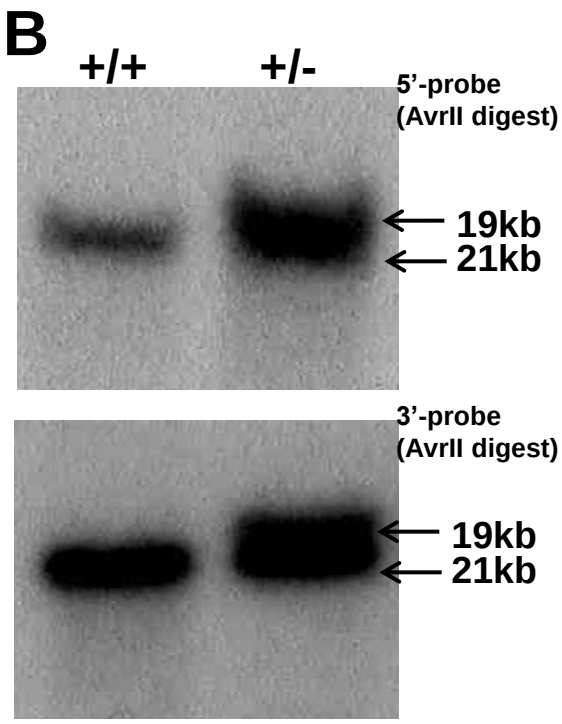

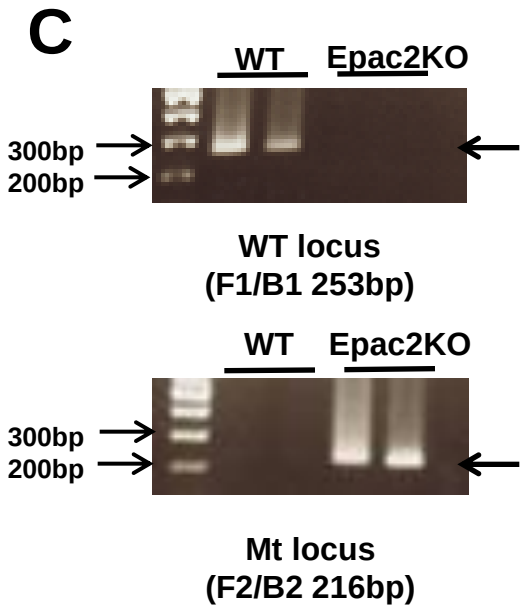

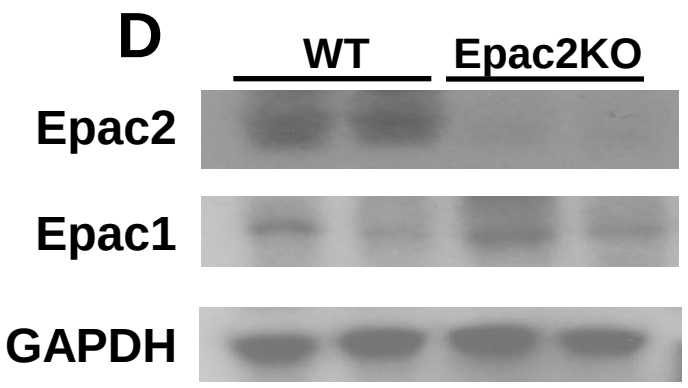

Supplemental Figure 21

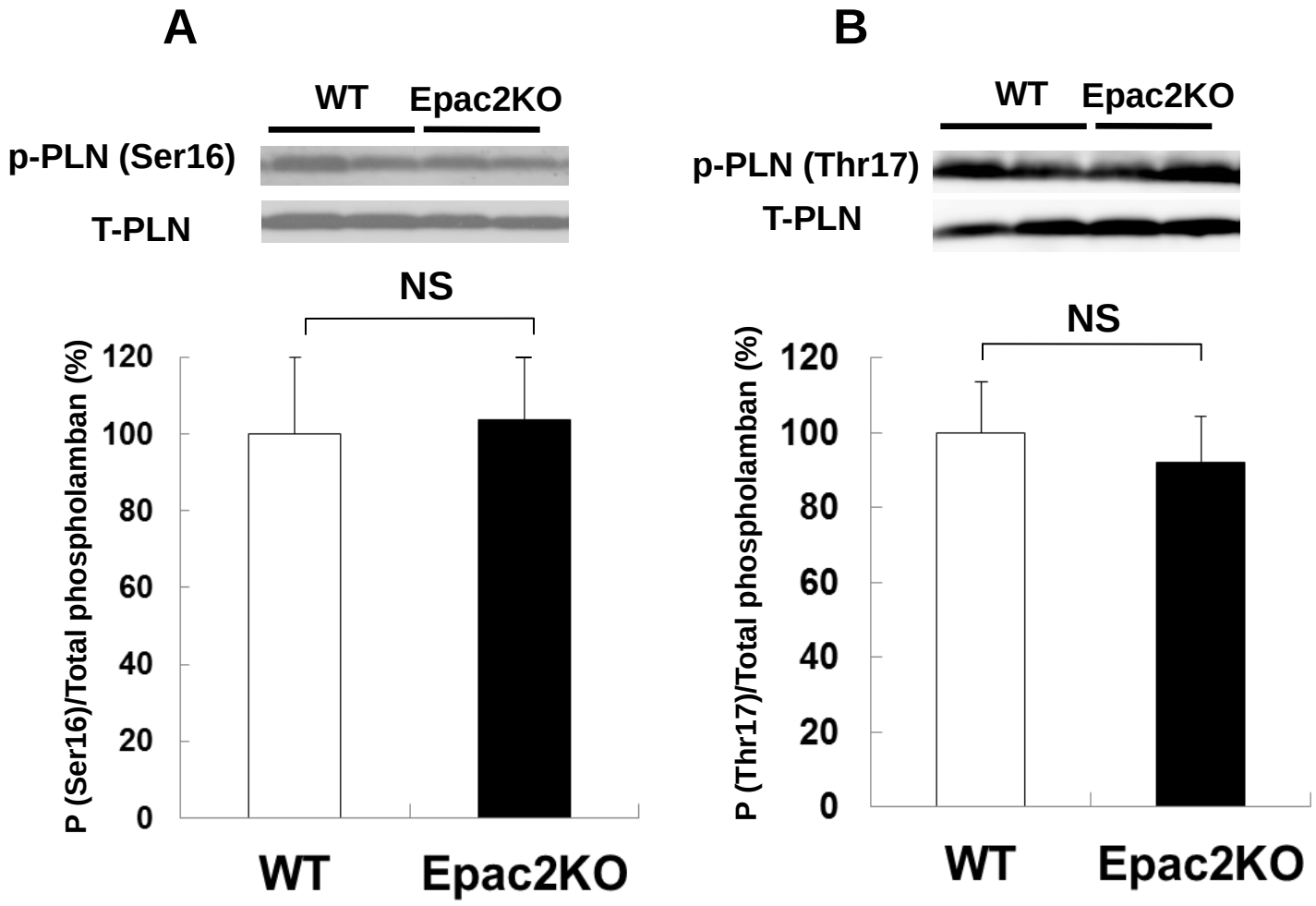

Supplemental Figure 22